The Canadian Mineralogist
Vol. 35, pp.1391-1414 (1997)

FLUID-INCLUSION VOLATILE ANALYSIS BY GAS CHROMATOGRAPHY: APPLICATION OF A WIDE-BORE POROUS-POLYMER CAPILLARY COLUMN TO THE SEPARATION OF ORGANIC AND INORGANIC COMPOUNDS

STEFANO SALVI[1]

Laboratoire de Minéralogie, Université Paul-Sabatier, 39, allées Jules-Guesde, F-31000 Toulouse, France
Laboratoire de Géochimie, Université Paul-Sabatier, 38, rue des Trente-Six Ponts, F-31400 Toulouse, France

ANTHONY E. WILLIAMS-JONES

Department of Earth and Planetary Sciences, McGill University, 3450 University Street, Montreal, Quebec H3A 2A7

ABSTRACT

Gas chromatographic analyses of the volatile content of fluid inclusions were carried out using a recently developed PoraPLOT® Q mega-bore capillary column (25 m × 0.53 mm, 20 μm film thickness, fused silica) and on-line crushing techniques during heating. For comparison, analyses were also conducted with a HayeSep® R packed column (10' × 1/8" 120 mesh, Ni alloy tubing), which is the column most widely used for the analysis of inclusion gases. The wide-bore PoraPLOT® Q capillary column is ideally suited for analyses at relatively high flow-rates needed in processing fluid-inclusion gases released into the gas chromatograph by on-line crushing. This column proved superior to the packed column in that it reduced retention times by at least half, allowed clean separation of N_2, CO_2, CH_4, and higher hydrocarbons up to at least C_6 paraffins, and greatly improved detection and accuracy of analyses for H_2O. Furthermore, using N_2 as a carrier gas, it is possible to analyze for Ar and H_2 to ~10^{-4} μmoles and ~10^{-5} μmoles, respectively. The latter gas could not be analyzed with the packed column. Optimum conditions were found to be a carrier-gas flow of 20 mL/min, and an oven temperature programmed to start at –20°C, subsequently raised (10°C/min) to 35°C and held for 10 min, then again raised (5°C/min) to 115°C. Runs lasted ~80 min. The PoraPLOT® Q capillary column was used to measure the composition of carbonic fluid inclusions in the peralkaline granite at Strange Lake, Quebec–Labrador. These inclusions were shown to contain heavy aliphatic hydrocarbons in proportions consistent with their production *via* a Fischer–Tropsch reaction involving Fe-oxide-catalyzed hydrogenation of magmatic CO_2 and CO.

Keywords: gas chromatography, fluid inclusion, hydrocarbon, volatile, hydrogen, analytical technique, Fischer–Tropsch, Strange Lake, peralkaline granite, Quebec, Labrador.

SOMMAIRE

La proportion des volatils contenus dans les inclusions fluides a été déterminée par chromatographie en phase gazeuse à l'aide de la colonne capillaire récente en silice PoraPLOT® Q (25 m × 0.53 mm, film de 20 μm d'épaisseur), et d'un dispositif chauffé d'écrasement en ligne. Pour comparaison, nous avons également analysé les mêmes échantillons en utilisant une colonne compactée HayeSep® R (10' × 1/8", 120 mesh, tuyaux en alliage de Ni), soit la colonne communément utilisée pour l'analyse de gaz dans les inclusions fluides. La colonne capillaire à grande capacité PoraPLOT® Q est idéale pour les flux élevés nécessaires pour ce type d'analyses et s'est avérée supérieure à la colonne compactée, du fait qu'elle diminue le temps de rétention de plus de la moitié. Elle permet ainsi une meilleure séparation entre le N_2, le CO_2, le CH_4 et les hydrocarbures lourds jusqu'aux paraffines C_6, et améliore grandement la détection ainsi que la précision des analyses de l'eau. De plus, en utilisant l'azote comme gaz d'entraînement, nous avons pu analyser l'argon et l'hydrogène à des teneurs de, respectivement, ~10^{-4} μmoles et ~10^{-5} μmoles. La proportion de l'hydrogène n'a pu être établie avec la colonne compactée. Les paramètres optimaux pour les analyses ont été déterminés comme suit: flux du gaz transporteur de 20 mL/minute et programme de chauffage débutant à –20°C avec augmentation de la température de 10°C/minute jusqu'à 35°C. Cette température et ensuite maintenue durant 10 minutes, puis augmentée à nouveau, cette fois de 5°C/minute jusqu'à 115°C. La durée d'une analyses est donc de 80 minutes, environ. La colonne capillaire PoraPLOT® Q a été utilisée pour mesurer la composition des inclusions fluides carboniques dans le granite hyperalcalin de Strange Lake (Lac Brisson), Québec–Labrador. Ces inclusions contiennent des hydrocarbures aliphatiques lourds, dont la production peut s'expliquer par une réaction de type Fischer–Tropsch, catalysé par des oxydes de fer, qui comporte une hydrogénisation de CO_2 et CO de provenance magmatique.

Mots-clés: chromatographie en phase gazeuse, inclusions fluides, hydrocarbures, volatils, hydrogène, techniques analytiques, Fischer–Tropsch, Strange Lake, granite hyperalcalin, Quebec, Labrador.

---

[1] *E-mail address*: salvi@lucid.ups-tlse.fr

INTRODUCTION

Gas chromatography has been employed for the analysis of volatile constituents of bulk samples of fluid inclusions for over thirty years (*e.g.*, Goguel 1963, Petersilie & Sørensen 1970, Mironova *et al.* 1973, Ypma 1974, Cuney *et al.* 1976). However, the technique has had limited application because of inadequate sensitivity, which has restricted analysis to major volatile components. Better techniques of extraction, superior detectors and the development of new gas chromatographic columns have greatly improved sensitivity, and as a result, it is now possible to detect gases at concentration levels as low as 10^{-6} μmoles. This sensitivity permits analyses of trace components comprising as little as 10^{-4} mol.% of the gas phase. The method thus enables detection of gases at lower levels than Raman spectroscopy (~1 mol.%), by far the most widely used method of analyzing fluid inclusion gases (*cf.* Rosasko *et al.* 1975, Delhaye & Dhamelincourt 1975, Pasteris *et al.* 1986, Chou *et al.* 1990). It also allows analysis of hydrocarbons other than methane, a feature that is generally not possible with Raman spectroscopy, because of strong interferences due to fluorescence of these compounds. Finally, it can be used to quantitatively analyze for H_2O, which also is not possible with Raman spectroscopy (*e.g.*, Roedder 1990).

Until recently, gas chromatographic analysis of fluid inclusions has generally proceeded in two steps. The gases were first released and collected, and then an aliquot of the captured gases was introduced into the chromatograph. Typical techniques of extraction consist of 1) stepwise decrepitation by heating (*e.g.*, Piperov & Penchev 1973), 2) grinding the sample in a stainless-steel or ceramic ball mill under vacuum (*e.g.*, Abell *et al.* 1970, Petersilie & Sørensen 1970, Roedder 1972), or 3) decrepitation under vacuum followed by gas separation (Behar & Pineau 1979, Welhan 1988). The decrepitation – extraction method has proven the most problematic as a result of thermal decomposition and heat-induced chemical reactions, which produce unreasonably high blank concentrations of the common inclusion components, CO_2, CH_4 and N_2. However, all these extraction techniques share another major weakness, namely that only a small proportion of the released volatiles can be collected for analysis. This significantly decreases the accuracy of the analysis and the ability to detect trace components.

Andrawes & Gibson (1979) designed an on-line crushing technique that greatly improved the quality of volatile extraction. The device consists of a piston–cylinder crusher operated by a hydraulic press, in which the sample chamber is heated to ≤300°C (*cf.* Andrawes *et al.* 1984). Their technique allows direct insertion of all the released gases into the gas chromatograph as the crusher is attached to the column. Also, heating of the sample chamber induces immediate release and dilution of volatiles in the carrier gas, which reduces chances of adsorption.

An important limitation of early gas chromatography was an inability to quantitatively analyze for water. Because of its polarity, H_2O was adsorbed onto the stationary phase contained in the packed columns available at that time. This problem was solved with the development, in 1966, of the Porapak® series of stationary phases, a type of apolar porous polymer consisting of divinyl benzene and diethyl benzene (Hollis 1966, Hollis & Hayes 1966, Merle d'Aubigné & Guiochon 1970, Gough & Simpson 1972), which allows elution of the strongly polar H_2O molecule. Since then, most gas chromatographic analyses of rock-derived gases have been carried out on these or similar columns. Separation of H_2O, CO_2 and light hydrocarbons up to C_3 has been typically carried out with Porapak® Q (*e.g.*, Cuney *et al.* 1976, Behar & Pineau 1979, Andrawes & Gibson 1979, Kreulen & Schuiling 1982, Kesler *et al.* 1986) or Chromosorb® 102 (*e.g.*, Smith *et al.* 1984, Kesler *et al.* 1986), whereas columns packed with molecular sieve 5 Å have been employed to resolve the $\pm N_2 \pm Ar \pm O_2 \pm CO \pm H_2$ composite peak (*e.g.*, Andrawes & Gibson 1979, Andrawes *et al.* 1984, Bray *et al.* 1991).

Bray & Spooner (1989, see also Bray *et al.* 1991, Bray & Spooner 1992) have taken the technique one step further by separating fluid-inclusion volatiles using a single column, albeit in two separate runs with different temperature programs. They used a 10' × $^1/_8$" outside diameter (OD) Ni alloy column, packed with HayeSep® R (100–120 mesh), a material similar to Porapak®, but with higher efficiency and inertness (*cf.* Pollock *et al.* 1984). Their system allows routine analysis of up to three samples a day for N_2, Ar, CO, CH_4, CO_2, C_2H_4, C_2H_6, C_2H_2, C_3H_6, C_3H_8, C_3H_4, C_4H_8 (isobutylene), COS, and H_2O, with a detection limit of less than 10^{-4} μmoles for major components (CO_2, CH_4, N_2) and down to less than 10^{-5} μmoles for unsaturated hydrocarbons (*cf.* Bray *et al.* 1991). In addition to these species, they reported separation of O_2 from standards, an unquantifiable peak for SO_2, and a few unresolved composite peaks of other C_4 species.

We have constructed a gas chromatographic system for on-line analysis of fluid inclusions, based largely on the design developed by Bray and Spooner at the University of Toronto. However, we have elected to use a wide-bore capillary column (25 m × 0.53 mm inside diameter fused silica) coated with PoraPLOT® Q (film thickness: 20 μm) instead of their HayeSep® column. The PoraPLOT® Q column has proved ideal for the analysis of volatiles in fluid inclusions. This column allows separation of permanent gases as well as light hydrocarbons up to at least C_6, and even some aromatic species, in a single run; it improves peak resolution (enhancing separation and potentially leading to lower limits of detection), and it greatly improves the quality of the H_2O peak, thereby increasing the accuracy of analyses. Furthermore, by using N_2 as carrier gas, it is possible to resolve H_2 (not possible with HayeSep® R); we were able to analyze this gas in fluid inclusions to levels of ~10^{-5} μmoles.

In this paper, we report the results of experiments using standard mixtures of gases as well as natural samples, and compare these to the results for the same samples using a packed column identical to that employed by Bray & Spooner (1989).

EXPERIMENTAL PROCEDURE

The instrument used in our analyses is a HP® 5890 Series II gas chromatograph manufactured by Hewlett-Packard, equipped with a micro-thermal conductivity detector. The oven temperature can range from –80°C (using liquid nitrogen) to 450°C in increments as low as 0.1°C/min. Control of the oven temperature is precise to within ±0.01°C of a setpoint. The analogue signals that constitute the output of the detectors are converted to digital data by a HP® 35900C dual-channel interface; this device accepts a signal voltage in the range –18 mV to +1 V. The data are subsequently transmitted to an HP® 3365 ChemStation®, a PC Microsoft® Windows™ operated computer code designed to manipulate and integrate chromatographic spectra.

At present, our gas chromatograph is configured to operate cryogenically down to temperatures of –40°C using liquid CO_2 as a coolant (lower temperatures are possible with this coolant, but one risks damage to the gas chromatograph). Cooling is achieved by allowing high-pressure liquid CO_2 (5000 kPa at 25°C) to enter the oven by means of an electronically controlled solenoid valve.

Of the several inlets available, we have chosen the split–splitless injector instead of the commonly used packed injector (*e.g.*, Bray *et al.* 1991), as it can be employed with all types of capillary columns and can be easily modified to function as an inlet for packed columns. In its present configuration, the injector is in the latter operational mode (Fig. 1), as wide-bore columns (see below) require the high flow-rates typical of packed columns.

System for the extraction of fluid-inclusion volatiles

The apparatus employed for volatile extraction consists of a heat-treated stainless-steel crusher, as modified by Bray & Spooner (1989) from an original design of Andrawes & Gibson (1979), operated by hydraulic ram (Fig. 2). It allows immediate release of the contents of the fluid inclusions to the carrier gas and their direct insertion into the HP® 5890. The basal block is heated, *via* two cartridge heaters, to ~120°C.

The upper portion of the crusher contains a cylindrical piston (*cf.* Fig. 2 for dimensions) and attaches to the lower portion *via* a threaded connection. A seal, where the two parts join, is provided by a silicon-rubber O-ring at the base of the upper block and one at the lower end of the piston. An additional O-ring is placed near the top of the piston to create a further seal to prevent contamination from the external atmosphere. Andrawes *et al.* (1984) used vacuum grease to lubricate the O-rings, but we did not attempt this, for fear of contaminating the column. The dead volume between the two O-rings on the piston (Fig. 2) is pressurized with ultra-high-purity zero-grade He, the same gas (from a different tank) used as the carrier. This practice provides added protection in case the sample chamber should leak, especially when the piston is lowered during crushing (*cf.* Andrawes *et al.* 1984). An oil pump is connected to the ram by a on–off valve. Just prior to analysis, this valve is in the "off" position, and the pump is loaded to about 30 to 35 MPa. Releasing this pressure by switching the valve "on" causes a sharp and sudden stroke of the ram on the piston, which crushes the sample. The gas chromatograph run is started synchronously. After analysis, the sample chamber is cleaned with compressed air and clean tissues.

The sample to be analyzed is fragmented to pieces between 0.75 mm and 2 mm in diameter, and is hand-picked. Sample cleaning is performed using doubly distilled H_2O to avoid any possibility of contamination from acids or organic solvents. Between ~0.5 g to 2 g of clean, dry material is loaded into the crusher. The cartridge heaters are switched on, and both sample and confining chambers are pressurized with a low flux of He (≤1 mL/min). Flushing in He overnight at temperatures above the boiling of water removes all air and H_2O that may be absorbed onto the sample.

Choice of column

The ability of a chromatographic system to separate complex mixtures depends almost entirely on the choice of column. A packed column consists typically of 0.5 m to 3 m of metal (stainless steel, Ni alloy) or glass tubing, generally has an internal diameter (ID) between ~2 mm and ~5 mm, and is loaded with stationary phases, porous polymers, or molecular sieves. Capillary columns usually comprise between 12 m and 100 m of coiled stainless steel or fused silica tubing of very small ID (the usual range is from 0.18 mm to 0.53 mm), and are coated with a μm-scale thickness of stationary phases or porous polymers (recently developed), molecular sieves, aluminum oxide or carbon. There are probably over a thousand different columns on the market today.

We initially installed a packed column identical to that used by Bray & Spooner (1989), *i.e.*, 10' × $^1/_8$" OD HayeSep® R (Ni alloy tubing, 100–120 mesh). Although, as discussed by Bray *et al.* (1991) and Bray & Spooner (1992), the column allows separation of the lighter volatiles, we found that the large width of

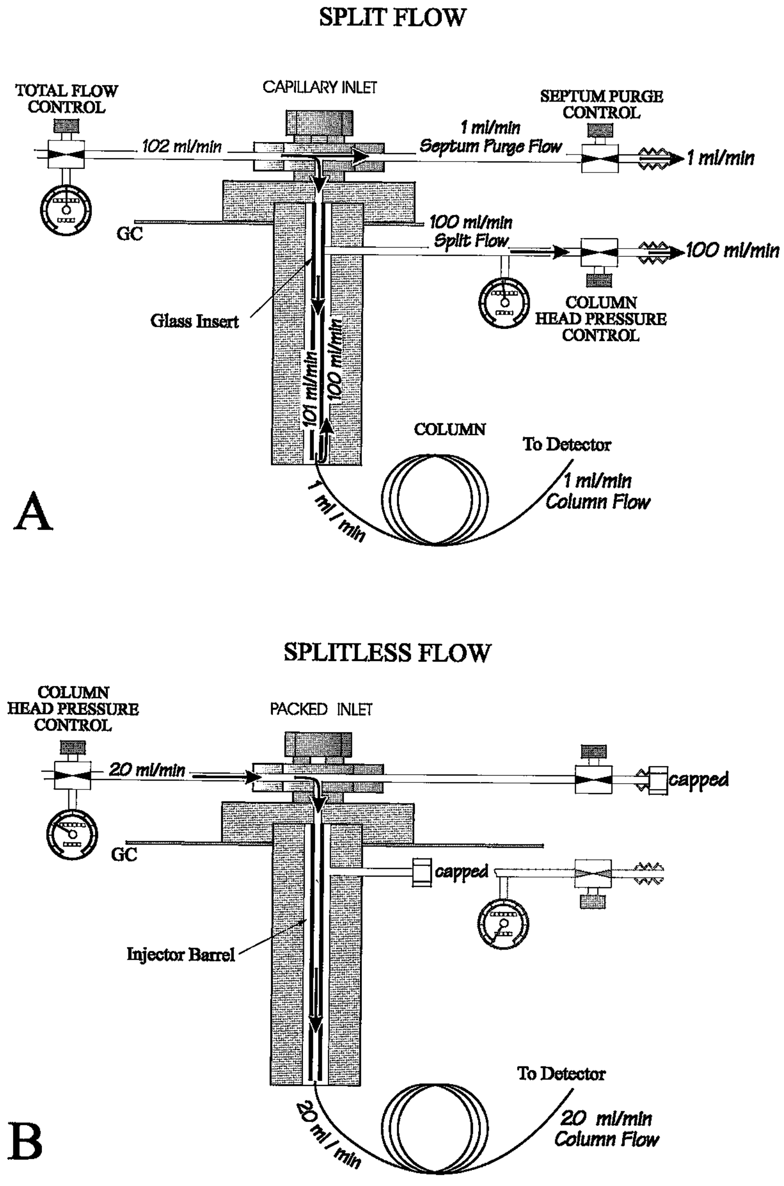

FIG. 1. Schematic cross-section of the split–splitless gas chromatograph inlet, depicting the gas flows in (A) the split configuration typically used with capillary columns, and (B) in the splitless mode, compatible with packed columns.

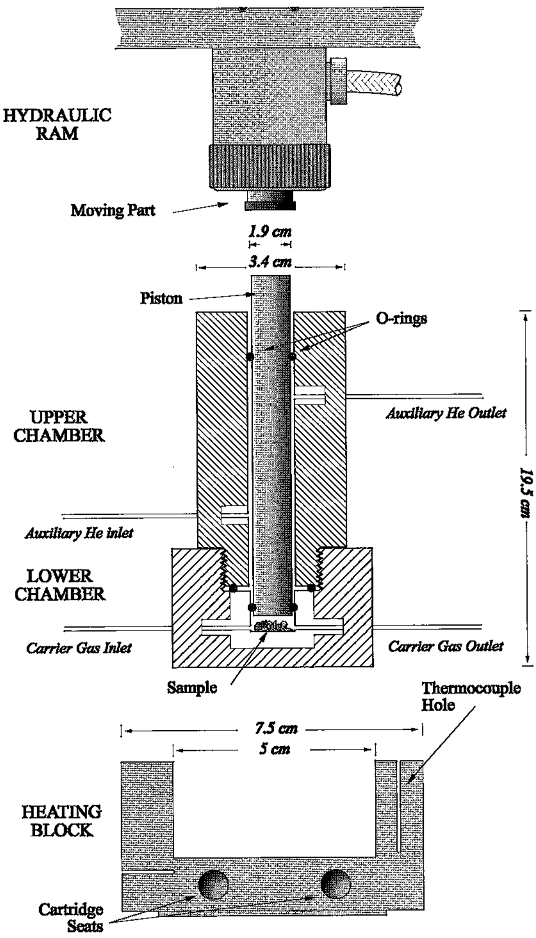

FIG. 2. Schematic cross-section of the crushing apparatus.

the H_2O peak masked part of the region that could be occupied by C_3 peaks, and that resolution of hydrocarbon species eluting after about 20 minutes of running time was very poor (see below). Varying the temperature program did not improve the quality of the analysis, as gains on some aspects represented losses in others, supporting the conclusion of Bray *et al.* (1991) that the 80°C isothermal run is the best compromise for this column. We therefore investigated alternative columns.

Analytical constraints quickly focused our attention on mega-bore capillary columns (0.53 mm ID), as they have the high capacity needed to separate volatile compounds as well as to deal with the introduction of the wide range of sample volumes, which characterizes analysis of fluid-inclusion volatiles. Furthermore, their wide bore allows operation with fast flow-rates (needed because of the large dead volumes inherent in the extraction system), thereby obviating the need to split the flow (*cf.* Fig. 1A), which would have proved very difficult with a crusher on line. The principal draw-back of mega-bore capillary columns was that they could not be used in the presence of H_2O. However, this limitation has recently been overcome with the development of the PLOT (porous layer open tubular) series of columns by Chrompack International. We have selected a 25 m × 0.53 mm inside diameter (ID), fused-silica PoraPLOT® Q column, which features a 20-mm-thick uniform layer of particles immobilized on the inner wall. This layer allows the separation of both polar and nonpolar volatile compounds, hydrocarbons and H_2O.

Choice of detector

The gas chromatograph used in this study is equipped with a micro-thermal conductivity detector (TCD) designed around a 3.5-µL cell, which improves detection limits by a factor of at least 50 with respect to conventional TCDs (Bray *et al.* 1991). Use of the micro-TCD also eliminates the need to pass the reference gas through a second column (*e.g.*, Behar & Pineau 1979) by using a solenoid valve that switches continuously between the carrier and the reference gas.

To analyze for hydrocarbons, we selected a photo-ionization detector (PID) over the commonly used flame-ionization detector because of lower limits of detection; because it is nondestructive, it can be connected in series with the TCD. The PID fitted to our system is the PI–52–02A model of HNU® Systems. Available ultraviolet lamps have energies ranging from 8.3 eV to 11.7 eV. The 10.2 eV lamp has the greatest sensitivity, but cannot detect low-molecular-weight compounds such as CH_4, C_2H_2, C_2H_4 and C_2H_6, which have higher ionization potentials. The 11.7 eV lamp, having the highest ionizing energy, is able to detect the widest range of molecular weights, but has an expected lifetime of only ~500 hours. Because of its construction, it should not be operated at temperatures greater than ~100°C. Because the C_2 hydrocarbons are poorly resolved by the TCD, but give excellent response on the 11.7 eV lamp, we fitted the PID with a 11.7 eV ultraviolet source. Methane ionizes at ≥12.98 eV, and therefore does not produce a linear response even on this lamp; however, it can be detected on the TCD at better than 10^{-4} µmoles. Many inorganic gases of interest ionize at >12 eV (N_2, CO, CO_2, CH_4, SO_2 and H_2O), and also cannot be detected with the PID. These are analyzed with the TCD.

Apparatus set-up

In a regular gas chromatograph, the carrier gas goes to a flow controller, which regulates the gas pressure and hence its flow through the column, and from this directly to the injector, where the sample is collected, before finally passing into the column. In this system (Fig. 3), the carrier gas (ultra-high purity He) is routed [by $^1/_8$" (3.2 mm) OD Cu tubing] to a three-way valve

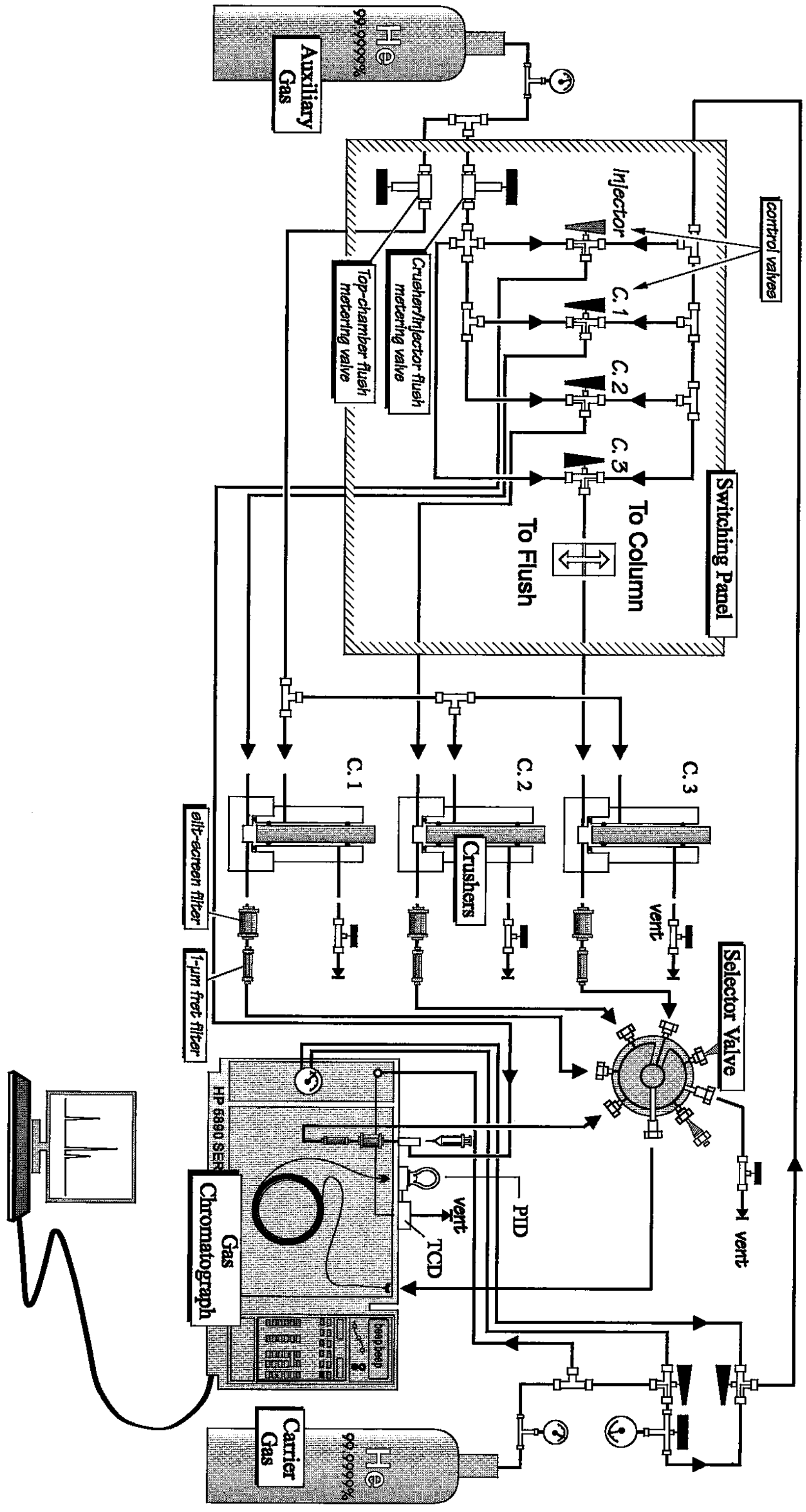

FIG. 3. A schematic diagram showing our gas chromatographic system.

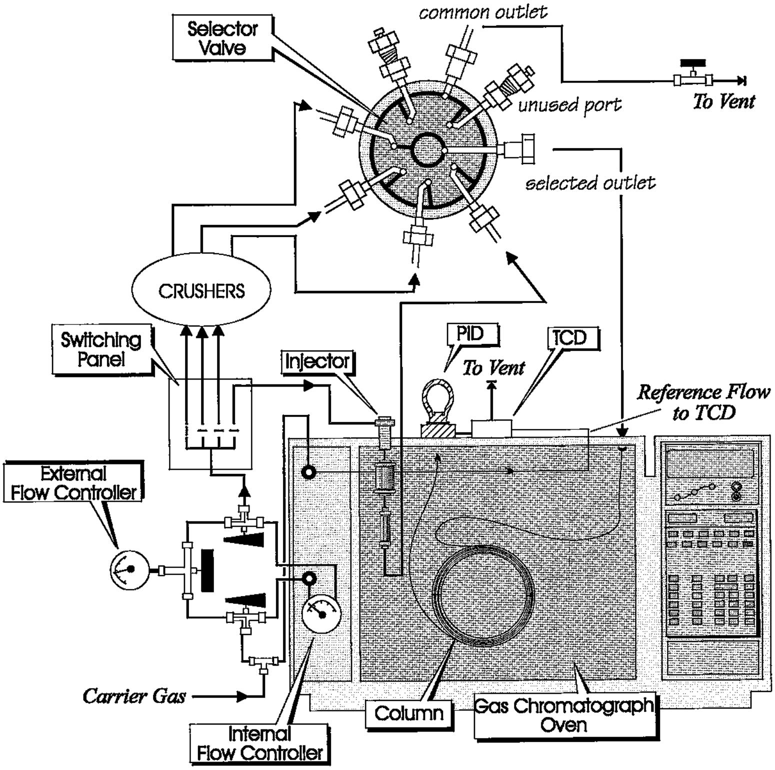

FIG. 4. A schematic diagram illustrating the operation of the 6-port valve used to direct one of the sample inlets to the gas chromatographic column. As one port is selected to allow gas flow to the column, all others continue purging to a common exit.

(Whitey® W1288 ball valve), which directs it either to the internal flow controller of the gas chromatograph, for capillary operation requiring split-flow mode (injector configured as in Fig. 1A), or to an external regulator (0 to 400 kPa), which mimics the packed flow controller (injector configured as in Fig. 1B). Both flow controllers are connected to a second three-way valve, which directs the selected flow to a switching panel, where it is split toward four three-way valves (control valves, Fig. 3). From here, the carrier gas can be directed to any of the three crushers or to the injector. All four injection ports are routed to a 6-port valve (zero-dead-volume Valco® SC6P–M–HC), which selects one of the entry ports while venting all others at a common exit (Fig. 4). The selected outlet is directed to the column. The tubing connecting each of these devices to the 6-port switching valve has to be exactly the same length in order to produce comparable retention-times between any of the crushers or the injector.

To prevent absorption of sample components on their way to the column, all connections down-flow from the crushers and the injector are made with Ni alloy tubing and Swagelok® stainless steel fittings; the 6-port selector valve was constructed with Hastelloy® C. This valve and the tubing connecting it to the gas chromatograph are heated to ~120°C to minimize condensation of higher boiling-point species.

To prevent rock particles and dust from damaging the selector valve and the column, a silk-screen particle filter (~200 μm pores) and a 1-mm fret filter are connected in series to the sample chamber outlets of the crushers. A similar pair of filters are fitted on the injector line, to keep flows equal (Fig. 3). Because of the delicate nature of the stationary phase in the PoraPLOT® column, additional protection for the column is provided by a 2.5 m × 0.53 mm ID particle trap, connected at the start of the column.

A second tank of ultra-high purity He (labeled "auxiliary gas" in Fig. 3) is used to provide the confining pressure in the upper portion of the crushers, and to supply He for flushing the crushing chamber in preparation for analysis (Fig. 3). Two metering valves (Whitey® 21RS2 needle valves) mounted on the switching panel direct the gas to the other end of the four control valves. This allows crushers (or injector or both) that are not on-line with the column to be flushed, at a flow rate regulated by the metering valve, with a stream of He identical to, but independent from, the carrier gas, which vents at the common exit of the 6-port selector valve. A shut-off valve fitted on this exit allows the plumbing system to be closed and the pressure to build up as needed. The second metering valve adjusts the flow to the top chambers of the crushers, where shut-off valves on the chamber outlets allow the system to be pressurized.

RESULTS

To evaluate the performance of the gas chromatographic system, we first carried out several runs without loading the sample chamber, then crushed material with physical properties similar to those of the samples that would be analyzed (usually quartz), but devoid of inclusions. Ideal candidates for such blanks are inclusion-free crystals of Brazilian quartz, and pure-silica laboratory glassware. These materials were fragmented, sieved, and cleaned exactly as would be regular samples (see above); prior to analysis, they were flushed overnight with He.

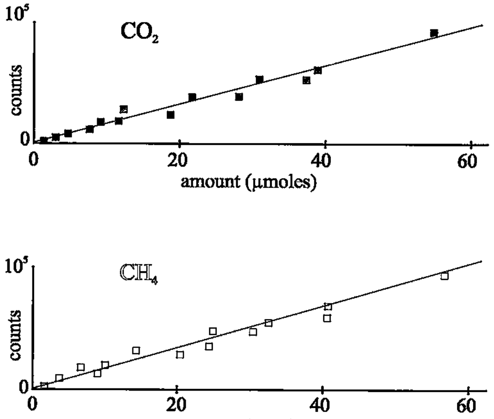

FIG. 5. Examples of calibration curves for volatile species created by analyzing several gas mixtures of known composition.

Experiments involving rock material were conducted using pegmatitic quartz from the Strange Lake peralkaline granite complex, Quebec–Labrador (Zajac *et al.* 1984, Miller 1986). These pegmatites were shown to contain methane- and higher-hydrocarbon-bearing fluid inclusions (Salvi & Williams-Jones 1992). Based on their fluorescence under ultraviolet illumination, the hydrocarbons may be unsaturated aliphatic or aromatic compounds (or both) (Salvi & Williams-Jones 1992).

TABLE 1. RETENTION TIMES AND OTHER INTEGRATION RESULTS FROM RUNNING A STANDARD GAS MIXTURE USING THE PACKED COLUMN (CF. FIG 6)

Sample Name: Mix 216;[†] Injected: 25 µl

Column: HayeSep R

Peak #	R. T.[‡] *(min)*	Area *(counts)*	Height *(counts)*	Width *(min)*	Area %[§]	Species
TCD						
1	2.7	2036500	244657	0.13	94.05	$N_2 + CO$
2	3.0	36300	2894	0.18	1.67	CH_4 methane
3	4.0	24200	2559	0.15	1.12	CO_2 C dioxide
4	5.2	23000	2100	0.17	1.06	C_2H_4 ethylene
5	6.0	19400	1700	0.17	0.90	C_2H_2 acetylene
6	6.2	26000	2030	0.19	1.20	C_2H_6 ethane
Total area = 2165300						
PID						
1	2.7	11000	1177	0.16	0.91	$N_2 + CO$
2	5.2	280000	25514	0.18	23.34	C_2H_4 ethylene
3	5.9	909000	69339	0.22	75.75	$C_2H_2 + C_2H_6$
Total area = 1200000						

[†] 1% each of CO, CO_2, CH_4, C_2H_2, C_2H_4, C_2H_6 in N_2

[‡] Retention times (R.T.) can vary up to ~±5% due to flow rate fluctuations

[§] Percentages calculated for each detector

Identification of peaks and standardization were achieved by injecting different amounts of known gas mixtures available commercially (Scott Specialty Gases Co., Plumsteadville, Pennsylvania), except for water, which was injected as saturated vapor at known temperatures and pressures. Identification of species was accomplished by comparing retention times. Calibration curves (Fig. 5), constructed by plotting the integrated peak-areas against the injected amounts of a species (known), were used to determine the amounts of the eluted gases.

Packed column

Initially, experiments were carried out using a 10' × $^1/_8$" OD Ni-alloy column packed with HayeSep® R (100/120 mesh). The injector was set up for the packed configuration (Fig. 1A) and heated to 120°C. The photo-ionization detector was set at ~105°C, hot enough to keep H_2O in the vapor state, yet below the recommended maximum operating temperature; the micro-thermal conductivity detector (TCD) was heated to 150°C. Although the latter detector could have been set to much higher temperature, the Hewlett-Packard instruction manual claimed greater sensitivity of the TCD if the detector body is maintained at low temperature. A convenient flow-rate of the carrier gas was determined to be 20 mL/min at 80°C, measured at the vent port of the TCD (*cf.* Fig. 4). For this flow rate, the optimal reference-gas flow to the TCD was 30 mL/min, again as recommended by Hewlett-Packard Co. for the best performance of the detector. As mentioned above, for the purpose of volatile analysis of fluid inclusions, a constant temperature of the oven of 80°C during runs proved to be the best compromise. Retention times (Tables 1, 2) were found to be slightly longer than those reported by Bray *et al.* (1991), probably due to the greater lengths of tubing connecting the crushers and injector to the column in our system.

TABLE 2. RETENTION TIMES AND OTHER INTEGRATION RESULTS FROM ANALYSIS OF QUARTZ FROM STRANGE LAKE USING THE PACKED COLUMN (CF. FIG 7)

Sample Name: 56-A-1; 1.3g, Crusher 1

Column: HayeSep R

Peak #	R. T.† *(min)*	Area *(counts)*	Height *(counts)*	Width *(min)*	Area %‡	Species	
TCD							
1	2.6	14300	1764	0.12	0.12	N_2	nitrogen
2	3.0	332600	40392	0.13	2.69	CH_4	methane
3	3.9	98000	10610	0.14	0.79	CO_2	C dioxide
4	6.2	70700	5564	0.20	0.57	C_2H_4	ethane
5	24.5	11841600	77735	4.79	95.73	H_2O	water
Total area =12357000							
PID							
1	2.7	2600	332	0.13	0.32	N_2	nitrogen
2	5.2	1200	117	0.17	0.15	C_2H_4	ethylene
3	6.2	182100	13821	0.21	22.78	$(C_2H_2?+)\ C_2H_6$	
4	19.7	561800	11692	0.72	70.30	C_3H_8	propane
5	43.9	3200	31	1.72	0.39	C_4H_{10}	butane
Total area = 799100							

† Retention times (R.T.) can vary up to ~±5% due to flow rate fluctuations

‡ Percentages calculated for each detector

Blanks run to simulate crush action with an empty sample chamber, *i.e.*, by just moving the piston, gave a flat signal for both TCD and PID detectors. Blanks using inclusion-free Brazilian quartz and fragmented pure-silica tubing also gave flat signals, except for a small unidentified hump at ~65 min in both quartz and Si tube runs. Bray *et al.* (1991) reported a similar unknown peak for their blank.

When analyzing mixtures of the lighter gases (Table 1), the first species to exit the column are $N_2 \pm CO \pm Ar \pm O_2$, which produce a composite peak at 2.7 min (Fig. 6). This peak, albeit much smaller, was also observed on runs of Strange Lake quartz (Fig. 7). Bray *et al.* (1991) reported the presence of the same peak in their 80°C runs, and used an oven temperature of –70°C to resolve it. They found that in all natural samples analyzed, the only species present was N_2. This is predicted by the extremely low fugacities of O_2, CO and Ar in nature (CO only attains significant fugacities at high temperatures, >600°C, and low $f(O_2)$: Eugster & Skippen 1967).

Methane elutes at 3.0 min, and CO_2 is detected at 4.0 min. As mentioned above, both gases give a negative response on the PID, but are well resolved by the TCD (Figs. 6, 7). The C_2 hydrocarbons elute next; although the PID is much more sensitive to these species than the TCD, if present in large amounts, they are also resolved by the latter detector. Interestingly, while the PID generates a peak for C_2H_4 (at 5.2 min) and a composite $C_2H_2 \pm C_2H_6$ peak at 6 min from running the standard mix 216 (Fig. 6), the composite peak is split by the TCD into peaks at 5.9 min and 6.2 min, representing C_2H_2 and C_2H_6, respectively. On the other hand, concentrations of these species in natural samples are rarely high enough to produce a signal on the TCD. Bray *et al.* (1991; see also Bray & Spooner 1992) did not report splitting of the $C_2H_2 \pm C_2H_6$ peak. This is possibly due to slight differences in the sensitivities of the detectors.

The next peak to appear on the TCD trace is H_2O at ~25 min (Fig. 7). Water produces a tailed peak, at least one order of magnitude wider than the earlier peaks. The skewness of the water signal most likely reflects absorption, followed by slow desorption, of H_2O onto the column phase. Chromatograms published in Bray & Spooner (1992) and in Thomas *et al.* (1990) obtained with the same packed column show very similar shapes for the H_2O peak. The PID has a nonlinear response to H_2O and, depending on the H_2O concentration, may give a negative peak of the same width as the equivalent positive peak from the TCD, or an even wider positive signal.

Most samples produced a n-propane (C_3H_8) peak on the front shoulder of the water disturbance on the PID trace, centered at 19.5 min (Fig. 7). Integration of this peak is problematic, firstly because at low concentrations it can be partly masked by the large H_2O peak, and secondly because the associated background is quite variable. Bray & Spooner (1992) reported detection of COS on the PID, at a retention time between that of C_2 and C_3 hydrocarbons, in samples from the Tanco granitic pegmatite (Manitoba) and the Boss Mountain molybdenite deposit (British Columbia). They also interpreted an SO_2 peak on the negative disturbance created by H_2O on the PID trace, but could not quantify it. We have not encountered these gases in the samples analyzed to date, and therefore did not run standards for them. However, it is reasonable to assume that these species also can be detected on our packed column.

After elution of water, the TCD signal is completely flat, whereas the PID inconsistently shows a small poorly shaped hump at ~45 min, tentatively assigned to a C_4 species, plus the unknown hump produced by the blanks at ~65 min (Fig. 7). It is evident from Figure 7 and Table 2 that the widths of the peaks increase rapidly with increasing retention-times, and that species eluting after H_2O have very low aspect-ratios, raising detection limits and drastically reducing the precision of their quantitative analysis.

After completion of an analysis (~80 min), the oven temperature is increased to 115°C (higher temperatures of the carrier gas could damage the PID lamp) and held for about 30 min, to speed up elution of any possible phase still remaining in the column. Next, the column temperature is returned to 80°C, and after thermal equilibration (~20 min), another run can be started.

Capillary column

Because of its high capacity, the 25 m × 0.53 mm ID PoraPLOT® Q column operates best at high flow-rates, which are compatible with the injector set-up in splitless mode (*i.e.*, as for packed columns, *cf.* Fig 1). Carrier-gas flow was 20 mL/min at 35°C, and reference-gas flow to the TCD was 30 mL/min, *i.e.*, the flow rates were similar to those used for the packed column. Detector body and injector temperatures were

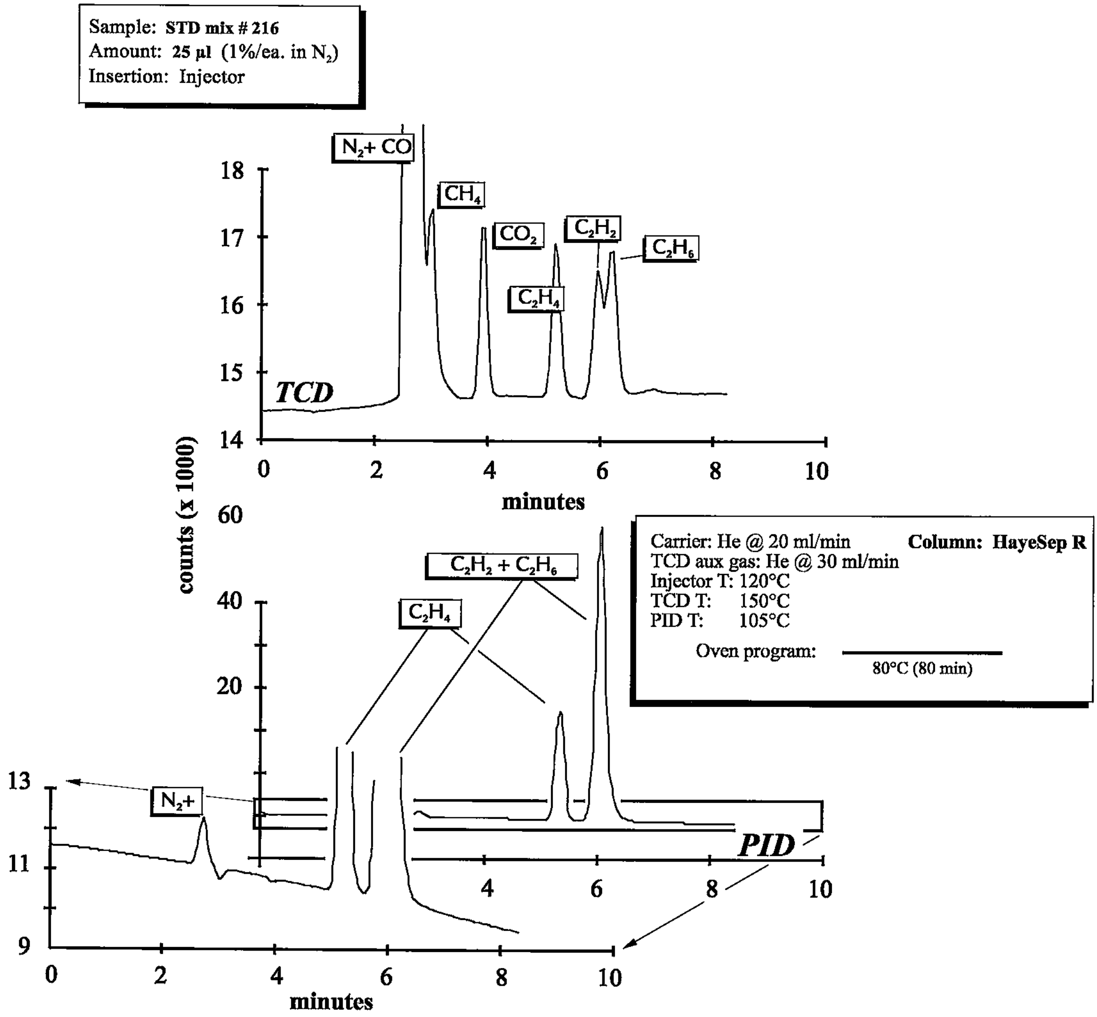

FIG. 6. Chromatograms showing the signals from the micro-thermal conductivity (TCD) and photo-ionization (PID) detectors for injection of 25 µL of standard mixture #216 into the HayeSep® R packed column.

also the same as with the packed column (see above). At an oven temperature of 80°C, *i.e.*, the setting used with the packed column, elution of the lighter gases was too fast, causing them to be insufficiently separated. After several runs, we adopted a temperature program that enabled separation of the light gases with relatively short total run-times; longer retention-times result in inferior definition of peaks. With this program, the oven is cooled to –20°C before the analysis is started, and 6.5 min into the run, after elution of CO_2 on the TCD, the oven temperature is increased at 10°C/min to 35°C, where it is held for 10 min to allow H_2O elution on a flat background (the TCD is much more sensitive to temperature fluctuations than the PID, Fig. 8). The temperature is then increased at 5°C/min to 115°C and left unchanged for ~40 min, when the run is stopped, after the C_6 gases are detected by the PID. Total running time is about 80 min.

Generally, the order of elution of species corresponds to the order of elution with the packed column, but retention times differ significantly (Tables 3, 4). The most striking improvement, using the capillary column, was the appearance of a number of peaks that had not been observed when the same samples were run on the packed column. Peak definition is much sharper, with widths $^1/_2$ to $^1/_{10}$ of those produced by the same species on the packed column (*cf.* Tables 2, 4). This greatly improved resolution, and allowed more precise

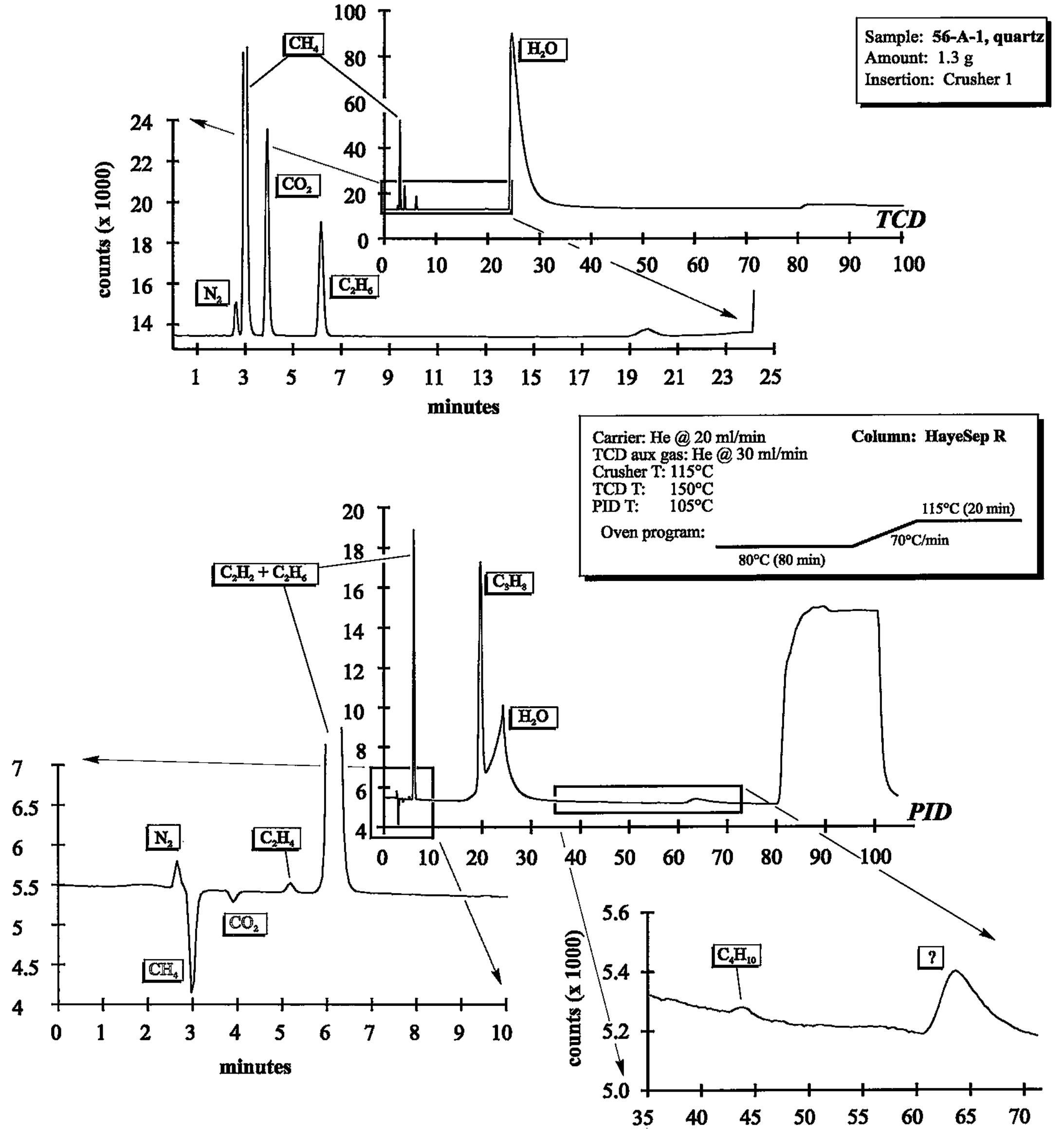

FIG. 7. Chromatograms showing the signals from the micro-thermal conductivity (TCD) and photo-ionization (PID) detectors of fluid-inclusion volatiles released by crushing 1.3 g of quartz from pegmatite in the Strange Lake peralkaline granitic complex. The analysis was carried out using the HayeSep® R packed column.

determination of peak areas. Finally, water generates a signal with a width:height ratio approximately one quarter of that observed on the packed column for similar concentrations, and does not produce nearly as large a tail, although it does not show a perfect gaussian shape (Fig. 9). Most importantly, with the packed column, we needed to inject at least 100 μL of water-saturated vapor in order to obtain a peak, whereas 20 μL at the same conditions are sufficient using the capillary column.

In contrast to the results obtained using the packed column, there were a number of extra peaks on the PID traces from empty crusher runs as well as from those in which Brazilian quartz and silica tubing were crushed. The most important of these are two unidentified peaks at 29.1 min and 31.6 min, and two more at 37.2 min

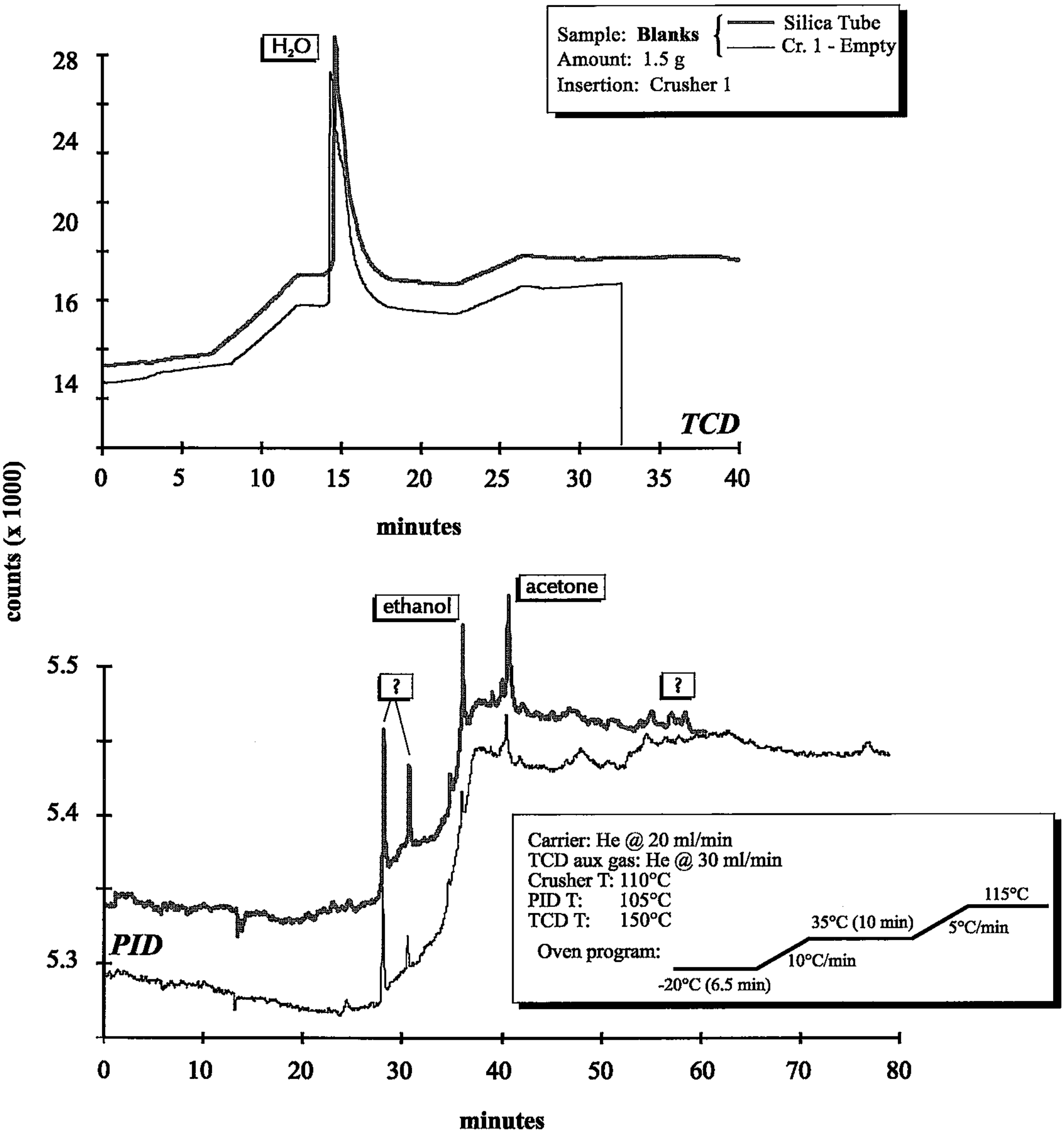

FIG. 8. Chromatograms showing the signals from the micro-thermal conductivity (TCD) and photo-ionization (PID) detectors, on running pure-silica tubing and empty-crusher blanks with the PoraPLOT® Q capillary column.

and 41.5 min, tentatively assigned to ethanol and acetone, respectively (Fig. 8). Andrawes *et al.* (1984) found that allowing the piston and the body of the crusher to come in contact produced significant H_2 and CH_4. Methane was not observed in our blanks (H_2 was not detected using He as carrier gas, see below), either because its concentration was below the detection limit of the TCD or because the material from which our crushers were constructed does not produce the same gases. However, since the contaminants found in our blanks occur independently of whether a sample is crushed or the piston is just moved without touching the shaft, we consider it likely that they originate from the silicone O-rings, rather than from degassing of the stainless steel. Moreover, the same peaks, although much smaller, are produced by inserting a needle through the silicone rubber septum in the injection port.

Small quantities of H_2O were detected on all blank runs and even by simply starting the temperature program. As suggested by Bray *et al.* (1991), this

TABLE 3. RETENTION TIMES AND OTHER INTEGRATION RESULTS FROM RUNNING A STANDARD GAS MIXTURE USING THE CAPILLARY COLUMN (CF. FIG 10)

Sample Name: Mix 216;[†] Injected: 3 µl

Column: PoraPLOT Q

Peak #	R. T.[‡] (min)	Area (counts)	Height (counts)	Width (min)	Area %[§]	Species	
TCD							
1	2.4	254000	40312	0.10	94.45	$N_2 + CO$	
2	2.9	2600	360	0.10	0.97	CH_4	methane
3	5.5	3100	391	0.10	1.16	CO_2	C dioxide
4	9.8	3000	449	0.11	1.11	C_2H_4	ethylene
5	10.2	2900	487	0.10	1.07	C_2H_2	acetylene
6	11.5	3400	547	0.10	1.25	C_2H_6	ethane
Total area = 268900							
PID							
1	2.3	500	66	0.12	0.80	$N_2 + CO$	
2	9.7	13200	1826	0.11	23.00	C_2H_4	ethylene
3	10.1	42000	6463	0.10	73.04	C_2H_2	acetylene
4	11.4	1800	276	0.10	3.16	C_2H_6	ethane
Total area = 57400							

[†] 1% each of CO, CO_2, CH_4, C_2H_2, C_2H_4, C_2H_6 in N_2

[‡] Retention times (R.T.) can vary up to ~±5% due to flow rate fluctuations

[§] Percentages calculated for each detector

probably reflects the presence of trace quantities of H_2O in the carrier gas. This fraction collects in the column during the subzero part of the run, and then is released at higher temperatures. However, unlike these authors, we did not detect CO_2 in our blanks, since the oven temperature is always well above the freezing point of CO_2. The amount of water contributed by the carrier gas is a very small proportion of the amount released from a sample, and was found not to vary significantly over a number of blank runs. This quantity can therefore be subtracted from the amount measured in a sample. A more precise analysis for H_2O can be obtained by performing a second crush of the sample at an oven temperature above the freezing temperature of H_2O. The results from the two crushes are normalized by using a species that can be measured in both runs (*e.g.*, CH_4).

On the segment of the run at –20°C, the TCD detects the $N_2 \pm CO \pm Ar \pm O_2$ peak at 2.4 min. CH_4 elutes at 2.9 min, and CO_2 at 5.6 min (Fig. 10). The PID detects C_2H_4, C_2H_2 and C_2H_6 at 9.9 min, 10.3 min and 11.6 min, respectively. Compared to runs with the packed column, acetylene and ethane are well isolated. Despite the fact that the oven temperature is increased at 10°C/min in this interval of the run, the background remains flat (Fig. 10), allowing clean resolution of these gases.

Water is separated at 14.5 min, on the 35°C plateau. Elution typically lasts about 2 to 4 minutes (*versus* 5 to 10 min with the packed column) depending on the concentration, after which, especially on the PID trace, the signal returns immediately to baseline background values. After elution of H_2O, data collection is stopped on the TCD, as species not yet eluted are detected on the PID. It is worth noting that if a species were to elute at the same time as water, the retention time of H_2O could be easily changed, and the two peaks neatly resolved, by simply holding the oven temperature below zero for a slightly longer or shorter time.

At the beginning of the second temperature program, the C_3 species elute on a flat background (Fig. 11; *cf.* Fig. 7). Although the C_3 hydrocarbons, propane (C_3H_8), propylene (C_3H_6), propadiene (C_3H_4) and propyne (C_3H_4) have been separated from standards mixes, C_3H_8, at 24.7 min, was the only C_3 species detected in the natural samples that were examined. The signal produced by elution of propane from the capillary column is much sharper than the same signal that was obtained from runs with the packed column; the ratio of peak width to peak height of propane in similar aliquots of sample 56–A–1 are at least three times greater for the packed column than for the capillary column.

TABLE 4. RETENTION TIMES AND OTHER INTEGRATION RESULTS FROM ANALYSIS OF QUARTZ FROM STRANGE LAKE USING THE CAPILLARY COLUMN (CF. FIG 11)

Sample Name: 56-A-1; 1.5g, Crusher 2

Column: PoraPLOT Q

Peak #	R. T.[†] (min)	Area (counts)	Height (counts)	Width (min)	Area %[‡]	Species	
TCD							
1	2.4	13500	2156	0.11	0.06	N_2	nitrogen
2	2.9	595900	92404	0.11	2.83	CH_4	methane
3	5.6	81900	9876	0.14	0.39	CO_2	C dioxide
4	11.5	133600	16843	0.13	0.63	C_2H_4	ethane
5	17.2	20265800	133116	1.84	96.09	H_2O	water
Total area =21091500							
PID							
1	2.4	500	64	0.13	0.03	N_2	nitrogen
2	9.9	600	84	0.12	0.04	C_2H_4	ethylene
3	10.3	500	77	0.10	0.03	C_2H_2	acetylene
4	11.5	126600	13999	0.15	8.45	C_2H_6	ethane
5	24.5	407500	19071	0.36	27.21	C_3H_8	propane
6	34.5	38100	2228	0.29	2.54	C_4H_{10}	isobutane
7	36.3	437000	34458	0.21	29.19	C_4H_{10}	n-butane
8	44.4	151700	6125	0.41	10.13	C_5H_{12}	isopentane
9	46.8	164300	7842	0.32	10.98	C_5H_{12}	n-pentane
10	66.8	48900	876	0.93	3.27	C_6H_{14}	isohexane
11	69.2	63000	967	1.09	4.21	C_6H_{14}	neohexane
12	75.0	58700	969	1.01	3.92	C_6H_{14}	n-hexane
Total area = 1504100							

[†] Retention times (R.T.) can vary up to ~±5% due to flow rate fluctuations

[‡] Percentages calculated for each detector

After elution of the unknown peaks that were produced by the blank runs (at 29.1 min and 31.6 min), isobutane (C_4H_{10}) elutes at 34.5 min, and at 36.3 min n-butane exits the column, followed immediately by the ethanol peak detected in the blank (see above). Isopentane and n-pentane (C_5H_{12}) elute after the oven has reached 115°C, at 44.5 min and 46.8 min, respectively (Fig. 11). As with the C_3 species, most of the C_4 and C_5 hydrocarbons have been separated from injections of standard mixtures on this temperature program, but only the C_4 and C_5 alkanes have so far been found in fluid inclusions. Butanes and pentanes produce high, sharp peaks (width/height ratios on the order of 10^{-4} to 10^{-5}) in all samples that, when previously analyzed on

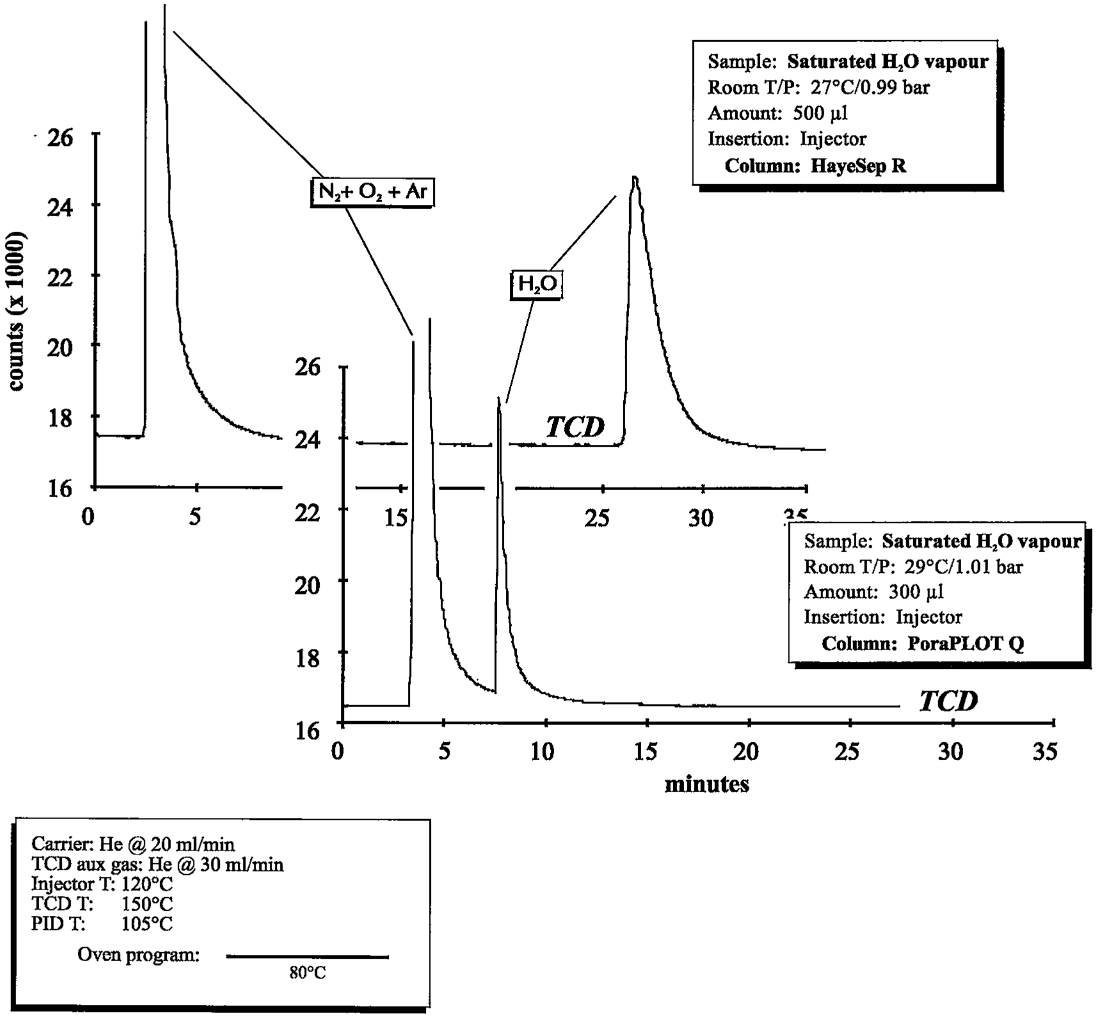

FIG. 9. Chromatograms showing the signals from the micro-thermal conductivity (TCD) of aliquots of H_2O-saturated vapor, analyzed at 80°C on the packed and capillary columns.

the packed column, were shown not to contain species heavier than propane. Because the detector was the same in both cases, it is evident that the PoraPLOT® Q capillary column permits a much improved detection of organic volatiles in inclusions over the HayeSep® R packed column.

Peaks at 66.8 min, 69.2 min and 75.0 min were observed for some samples. The last peak corresponds to n-hexane (C_6H_{14}), and although the other two are uncalibrated, they are tentatively assigned to isohexane and neohexane, respectively, on the basis of their boiling points. The poorer shape (width/height ratios $\geq 10^{-3}$) of the hexane signals is due to the late elution of these isomers and can be improved by running the samples isothermally at 115°C, which shortens retention times of these species to ~30 min. After the hexanes exit the column the run is stopped, at about 80 min, and the oven is returned to –20°C. Because of the nature of its construction material, this column reaches thermal equilibration with the oven almost immediately, which is convenient, especially when making subambient runs.

Heavier aliphatic and some aromatic hydrocarbons (*e.g.*, benzene, chlorobenzenes, toluene) also were separated on this column at 115°C, but their retention times are extremely long, causing very wide peaks ($\gg$5 min), which drastically limits detectability. This could be improved by fitting the PID with the 10.2 eV

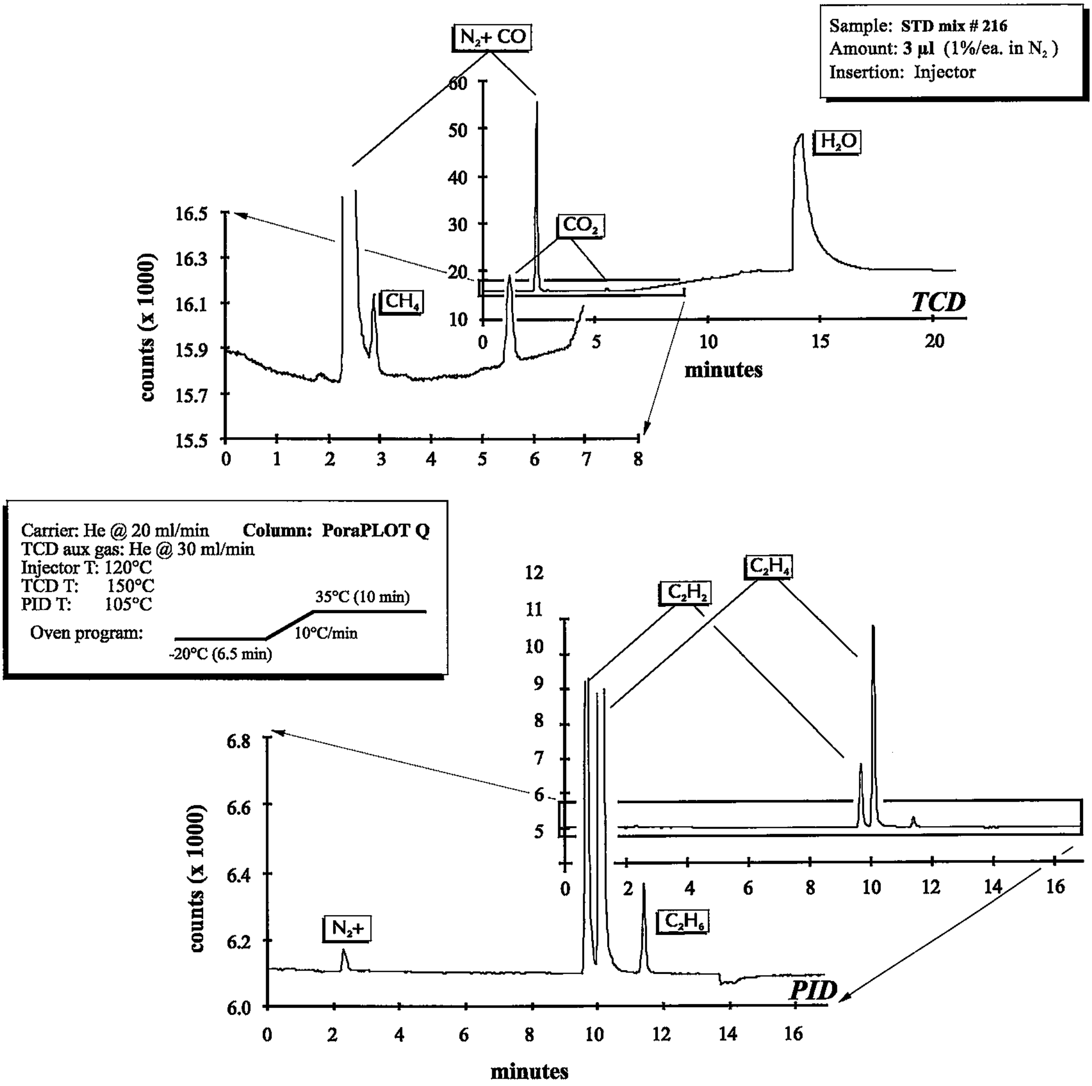

FIG. 10. Chromatograms showing the signals from the micro-thermal conductivity (TCD) and photo-ionization (PID) detectors after injection of 3 µL of standard mixture #216, into the PoraPLOT® Q capillary column.

lamp, which would allow an oven temperature of up to 300°C, and reduce dramatically the elution times of species with boiling points higher than ~100°C (*e.g.*, octane b.p. = 125°C), as well as provide at least a ten-fold increase in detector sensitivity for aromatics (*cf.* Driscoll & Duffy 1987). However, as mentioned earlier, the 10.2 eV lamp cannot detect the C_2 alkanes.

Analysis for hydrogen

Analysis of samples for H_2 by gas chromatography has been problematic owing to peak overlap with N_2, Ar, CO and O_2, and poor retention of this gas using porous polymer columns. Some authors have tried to resolve this problem by analyzing for H_2 using molecular-sieve-packed columns (*e.g.*, Andrawes & Gibson 1979), and although H_2 is detected at low concentrations with such columns, most other gases cannot be detected at the required levels. Consequently, the result for H_2 generally cannot be related to those for the remaining gases, which must be analyzed on another column.

We succeeded in analyzing for H_2 with the PoraPLOT® capillary column by changing the carrier

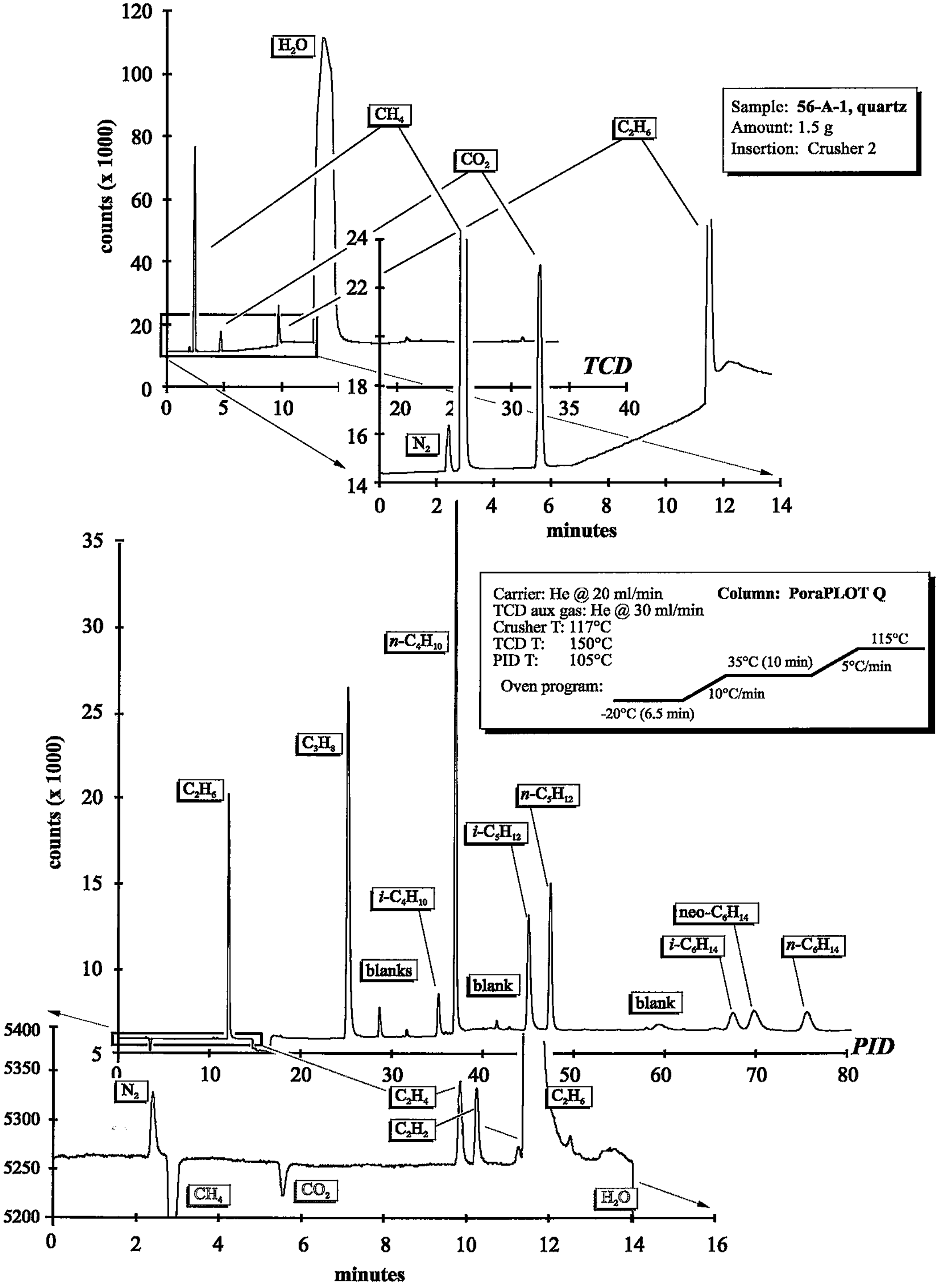

FIG. 11. Chromatograms showing the signals from the micro-thermal conductivity (TCD) and photo-ionization (PID) detectors of fluid-inclusion volatiles released by crushing 1.5 g of quartz from pegmatite of the Strange Lake peralkaline granitic complex. The analysis was carried out using the PoraPLOT® Q capillary column.

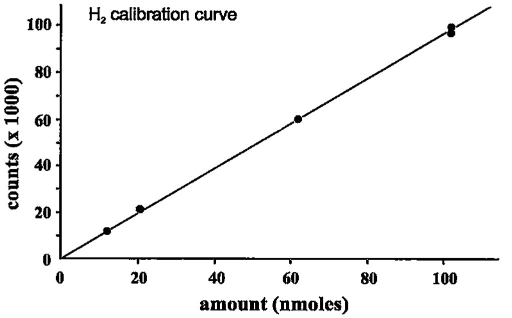

FIG. 12. A plot of measured peak areas *versus* different amounts of H_2 injected from standard mixtures. The line has a slope of 1.

to N_2. These two species differ in thermal conductivity by one order of magnitude, and thus the TCD is able to detect very low concentrations of H_2 (Fig. 12). In contrast, He and H_2 have very similar thermal conductivity, making detection for H_2 very poor with He as the carrier gas. The problem of N_2 and H_2 peak overlap is resolved by using N_2 as the carrier gas. Use of this carrier also allows H_2 to be separated from Ar, because Ar produces a peak with inverted polarity. The detection limit for CO is ~5 × 10^{-2} µmoles with N_2 as the carrier, making it essentially undetectable in fluid inclusions. Finally, the extremely low partial pressure of O_2 in even the most oxidizing hydrothermal fluids, rule out the possibility of it contributing to the H_2 peak.

Figure 13 shows chromatograms for sample TTR–22 collected with the TCD using He and N_2 as carrier gases. The peak at 2.4 minutes with He as the carrier is due to N_2, possibly with a small contribution from H_2, whereas the same peak with N_2 as the carrier is due entirely to H_2. Although all peaks with N_2 as the carrier, except Ar, are negative (due to the low thermal conductivity of N_2), the TCD showed a good linear response during calibration for most species analyzed. An exception is CO_2, which can only be analyzed to ~10^{-2} µmoles. Changing the carrier gas did not seem to have an effect on PID sensitivity (Fig. 14). The quantities of H_2 (and Ar) analyzed with N_2 as the carrier can therefore be related to the bulk composition of the gas analyzed with He as the carrier, by normalizing the H_2 content against those of species such as CH_4 or C_2H_6, which are detected with both carrier gases.

REPRODUCIBILITY OF GAS CHROMATOGRAPHIC ANALYSIS

In order to test reproducibility of the bulk analysis, we performed repeat analyses of sample 56–A–1 using He as the carrier gas. The sample was cut in half, and each portion treated as a separate sample throughout the whole procedure of sieving, picking, cleaning, and analyzing. In addition, we weighed different amounts for the two splits (0.41 g and 1.52 g), and did the analyses about one month apart.

The analyses of each portion of the sample, calculated both as absolute concentrations and normalized as percentages, together with the standard deviations, are listed in Table 5, and are shown graphically in Figure 15. Overall, the agreement between the two splits is very good, considering all the variables involved. Most compounds reproduced to ±15 mol.%, and for the more abundant components, *i.e.*, CH_4 and CO_2, the error was less than one order of magnitude smaller than the reported value. The largest discrepancy between the two analyses was for acetylene (C_2H_2), which yielded 0.012 and 0.056 mol.% in splits 1 and 2, respectively. The poor reproducibility of acetylene analysis could be due to concentrations close to its detection limit.

APPLICATIONS TO GEOLOGICAL PROBLEMS

Reduced gases in alkaline igneous rocks

Carbonic gas is a very common constituent of the volatile phase in magmas and is dominated by oxidized species (*i.e.*, CO and CO_2) in both volcanic and intrusive environments (*e.g.*, Gerlach 1980, Roedder & Coombs 1967, Holloway 1976); these species are also thought to constitute the principal form of volatile carbon in the mantle (*e.g.*, Pasteris & Wanamaker 1988). On the other hand, reduced carbonic species have been reported from inclusion fluids in silica-undersaturated alkaline rocks, *e.g.*, the McClure Mountain in Colorado: Heinrich & Anderson (1965), the Lovozero massif in the Kola Peninsula: Petersilie & Sørensen (1970), the Ilímaussaq intrusion in southwest Greenland: Petersilie & Sørensen (1970), Sobolev *et al.* (1970, 1974), Konnerup-Madsen *et al.* (1979, 1985), Konnerup-Madsen (1984), and more recently, from inclusion fluids in peralkaline granites, *e.g.*, the Strange Lake granitic pluton in Quebec–Labrador: Salvi & Williams-Jones (1990, 1992, 1997). These gases have been

TABLE 5. CONCENTRATIONS (ABSOLUTE AND NORMALIZED TO 100) AND STANDARD DEVIATIONS, σ, FOR THE VOLATILE CONTENT OF FLUID INCLUSIONS IN TWO SPLITS OF SAMPLE 56-A-1

		yields (nmoles)		moles %		
		split 1	split 2			
	(g crushed)	(1.5)	(0.4)	split 1	split 2	σ
N_2	nitrogen	3.1	0.6	0.44	0.45	0.01
CH_4	methane	569.4	113.2	80.44	83.22	1.96
CO_2	C dioxide	58.1	11.2	8.22	8.20	0.01
C_2H_4	ethylene	0.03	0.01	0.004	0.003	0.001
C_2H_2	acetylene	0.08	0.08	0.012	0.056	0.031
C_2H_6	ethane	60.3	8.8	8.34	6.50	1.30
C_3H_8	propane	12.0	1.4	1.70	1.05	0.46
i-C_4H_{10}	isobutane	0.6	0.1	0.08	0.06	0.02
n-C_4H_{10}	n-butane	4.3	0.5	0.61	0.36	0.17
n-C_5H_{12}	n-pentane	1.2	0.2	0.17	0.12	0.04

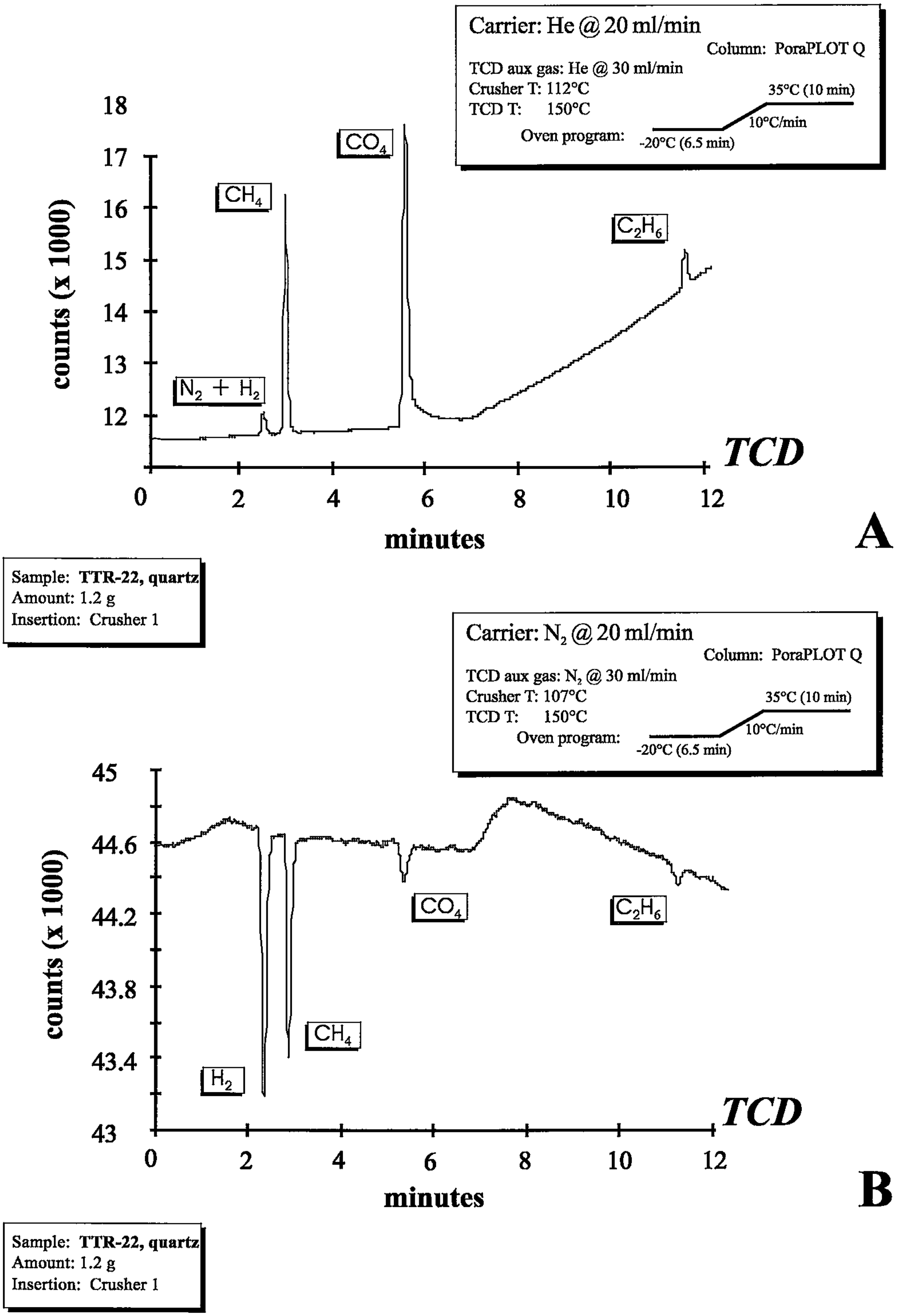

FIG. 13. Chromatograms showing the response of the micro-thermal conductivity detector (TCD) to gases released from crushing two aliquots of quartz from sample TTR–22 using (A) helium and (B) nitrogen as carrier gases.

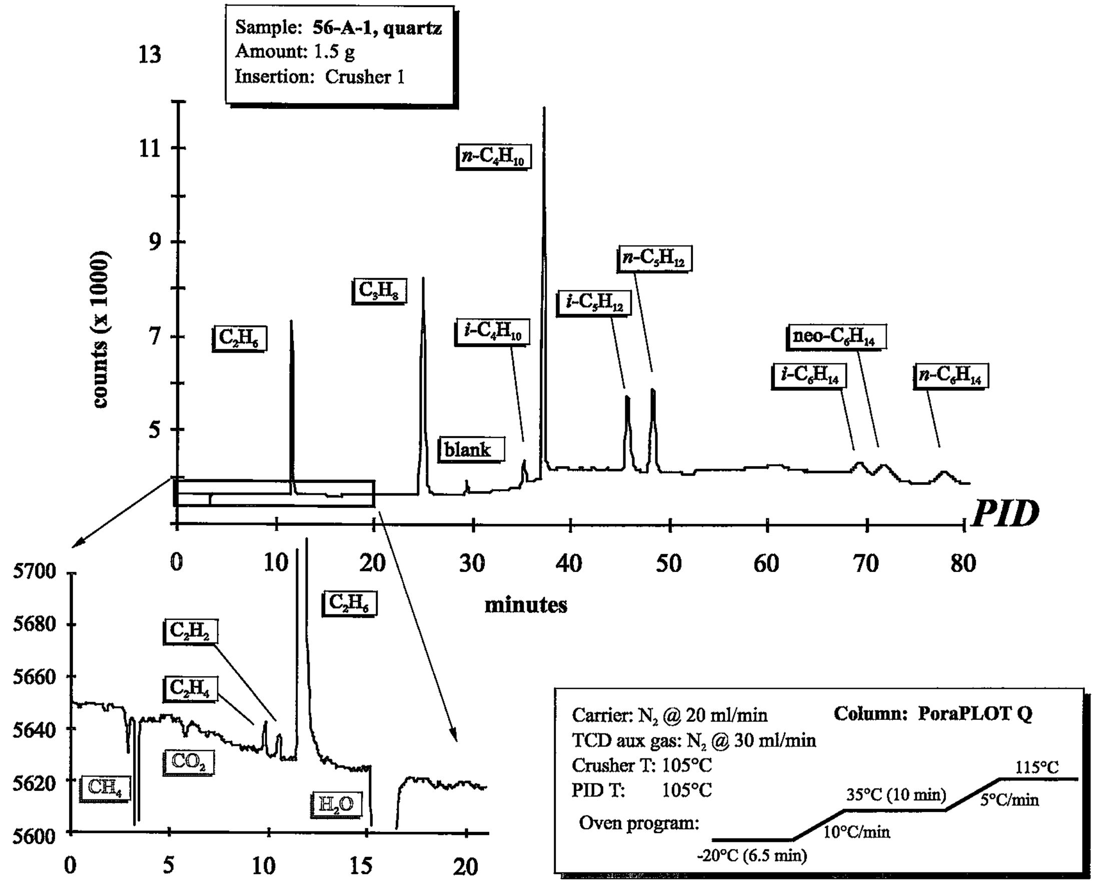

FIG. 14. A chromatogram showing the response of the photo-ionization detector (PID), using nitrogen as the carrier gas, to gases released from crushing quartz from sample 56–A–1, Strange Lake peralkaline granitic complex.

shown to be dominated by methane and to contain heavier hydrocarbons, unusually rich in hydrogen and containing significant nitrogen. However, quantitative analyses have only been possible for hydrocarbons up to C_3, and hydrogen has generally not been determined.

Most authors, proposing an igneous source for the carbonic fluids, envisage separation of a high-temperature (>400°C, and possibly >600°C) CO_2-bearing fluid from the magma, which transforms to methane on cooling along a path buffered by the rock to QFM redox conditions (*e.g.*, Gerlach 1980, Kogarko *et al.* 1987, Nivin *et al.* 1995). This theory satisfactorily explains the production of methane; however, it does not explain how hydrocarbons heavier than methane form in this environment (CH_4 is very much more stable than the other reduced-carbon-bearing species), nor, to our knowledge has the problem of the origin of the higher hydrocarbon species ever been systematically addressed. It has been tacitly assumed that the higher hydrocarbons derive from methane by condensation on cooling, without evidence of whether this is possible or how it might occur (*e.g.*, Konnerup-Madsen *et al.* 1988).

Pegmatites and adjacent altered peralkaline granites of the Strange Lake complex contain primary immiscible aqueous and carbonic fluid inclusions. On the basis of microthermometry, their strong fluorescence under ultraviolet illumination and results of Fourier-transform infrared spectroscopic analyses, the carbonic fluid inclusions were interpreted to consist dominantly of methane and higher hydrocarbons. However, it was not possible to identify the higher hydrocarbon species by these techniques. We therefore ran samples from pegmatites and granites using the gas chromatographic system described above with the PoraPLOT® Q column (*e.g.*, Fig. 11). The carbonic phase released by crushing these inclusions consists of about 69% methane, 19% hydrogen, 7% heavier hydrocarbons (in decreasing order of abundance, C_2H_6, C_3H_8, n–C_4H_{10}, n–C_5H_{12}, C_2H_2, i–C_4H_{10}, C_2H_4, i–C_5H_{12}, n–C_6H_{14}, i–C_6H_{14} and *neo*–C_6H_{14}), 3% CO_2 and 2% N_2 (Salvi & Williams-Jones 1997). These compositions are similar to those

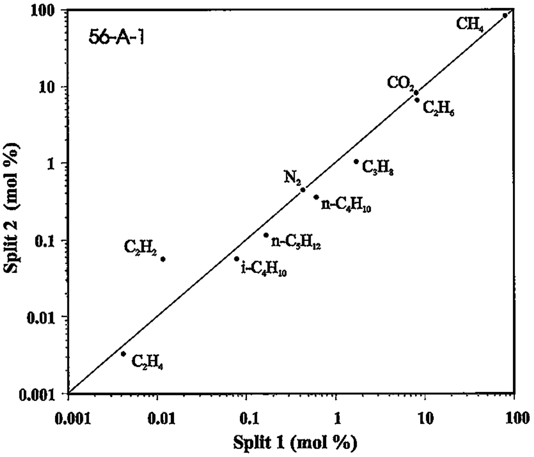

FIG. 15. Logarithmic plot of species concentration expressed as mol.%, for two separate splits of sample 56–A–1. The diameter of the dots corresponds to an error of about 5%, and the line has a slope of 1.

reported in the literature for the Ilímaussaq, Khibina and Lovozero intrusions. Thermodynamic calculations were carried out to test whether the carbonic species are at equilibrium in the proportions present in the inclusions (Salvi & Williams-Jones 1997). Such calculations show that the heavier hydrocarbons and hydrogen could not have coexisted at equilibrium in the proportions measured, at any P, T or $f(O_2)$ condition in the range independently estimated for the Strange Lake hydrothermal system, either prior to or after entrapment, nor could they have formed by reaction of the aqueous fluid with graphite. Instead, we propose that the higher hydrocarbon species in the Strange Lake fluid inclusions, and in other alkaline complexes, were produced by the disequilibrium reactions:

$$nCO + (2n+1)H_2 \quad C_nH_{2n+2} + nH_2O$$
$$nCO_2 + (3n+1)H_2 \quad C_nH_{2n+2} + 2nH_2O$$

in a manner similar to the Fischer–Tropsch (F–T) synthesis, which is used industrially to convert coal to petroleum in the presence of a Group VII metal or metal oxide catalyst (Anderson 1984). This interpretation is supported by the fact that the ratios of the mole fractions of pairs of progressively longer-chain hydrocarbons obey the Schulz–Flory law (Salvi & Williams-Jones 1997), which states that in a Fischer–Tropsch synthesis, the molecular ratios of hydrocarbons with successively higher carbon numbers are constant ($C_{n+1}/C_n = C_{n+2}/C_{n+1}$) (*cf.* Anderson 1984). Although the magma is the obvious source for the CO$_2$ or CO needed to produce the hydrocarbons, equilibrium calculations indicate that the exsolved gas will contain negligible H$_2$ at the temperature and $f(O_2)$ conditions interpreted for degassing (500° to 600°C; 2 to 3 log units below QFM: *cf.* Salvi & Williams-Jones 1992). Therefore, we propose that H$_2$ was produced during subsolidus alteration of sodic amphibole to aegirine as a result of interaction of the granite with fluids released from the pegmatite-forming magma *via* the reaction:

$$\underset{\text{arfvedsonite}}{3Na_3Fe^{2+}{}_4Fe^{3+}Si_8O_{22}(OH)_2} + 2H_2O \rightarrow \underset{\text{aegirine}}{9NaFe^{3+}Si_2O_6}$$
$$+ \underset{\text{magnetite}}{2Fe_3O_4} + \underset{\text{quartz}}{6SiO_2} + 5H_2$$

or

$$3Na_3Fe^{2+}{}_4Fe^{3+}Si_8O_{22}(OH)_2 + H_2O \rightarrow 9NaFe^{3+}Si_2O_6$$
$$+ \underset{\text{hematite}}{3Fe_2O_3} + 6SiO_2 + 3H_2$$

and that the Fe oxide produced by this alteration catalyzed the hydrocarbon synthesis.

Other geological environments

Reduced carbon interpreted to be of abiogenic origin has also been documented in seeps and plumes as well as in fluid inclusions from ultramafic rocks, both on the seafloor and on land (*e.g.*, Charlou & Donval 1993, Kelley 1996). An increasing number of such observations is causing investigators to suggest that abiogenic production of hydrocarbons could represent a far more important process than previously thought, and that CH$_4$ created during serpentinization could affect the redox state of carbon in a large proportion of the earth crust. A recently published experimental study on serpentinization of olivine under hydrothermal conditions (Berndt *et al.* 1996) has confirmed that H$_2$ liberated during this process reacts with CO$_2$ to produce methane. In addition to CH$_4$, gas chromatographic analyses of their run products has allowed determination of the proportions of heavier hydrocarbons. By observing that the hydrocarbons produced in their experiments had a Schultz–Flory distribution, these authors have shown that these gases were synthesized by a magnetite-catalyzed F–T process, in a manner similar to that described in the previous section for alkaline rocks. It is therefore evident that analyses of fluids circulating in ultramafic rocks must include determination of reduced hydrocarbon species, and that routine on-line gas chromatographic analyses of these rocks could prove important.

Another application of gas chromatographic analyses of fluid inclusions is the estimate of redox conditions (Halter *et al.* 1998). This can be accomplished by using CO$_2$/CH$_4$ values in the fluids obtained by gas chromatographic analyses and the reaction:

$$CO_2 + 2H_2O = CH_4 + 2O_2$$

assuming unit activity for H$_2$O and a correction factor for the temperature difference between entrapment and analysis of the fluid given in Dubessy (1984). With this technique, Halter *et al.* (1998) were able to calculate the $f(O_2)$ conditions prevailing during greisenization at the East Kemptville tin deposit in Nova Scotia, and show that the oxidation state of the greisenizing fluid decreased with alteration intensity to a minimum value between the NNO and QFM buffers in the most mineralized quartz–topaz greisen, where the highest grade ore is located. This interpretation is consistent with the $f(O_2)$ data obtained independently from chemical changes in rock composition (Halter *et al.* 1996).

The gas chromatographic system described in this paper also could have environmental applications. In a Raman spectroscopic study showing anomalous contents of hydrogen in fluid inclusions in the Leine anhydrite evaporites (Germany), Prohl *et al.* (1997) have noted that fluid inclusions in K-bearing hydrous minerals (*e.g.*, carnallite) contained higher amounts of H_2 than any other phase. They suggest that radioactive decay of ^{40}K causes radiolysis of H_2O in the mineral structure which, in turn, liberates free hydrogen gas. This phenomenon has applications to problems related to the disposal of radioactive waste in evaporite beds, as decay-induced corrosion of containers would most likely be accompanied by production of large amounts of hydrogen. Characterization of H_2-bearing inclusions in these rocks would help to investigate their hydrogen permeability over geological time, and thus allow assessments on long-term viability of radioactive-waste-disposal sites in rock salt. The gas chromatographic system would be a more useful tool than Raman spectroscopy for this purpose. The latter technique is bound by much higher limits of detection for H_2, and is restricted to samples that do not contain heavy aliphatic or aromatic (*i.e.*, fluorescing) hydrocarbons, which are a common occurrence in evaporites sequences.

Highly reduced conditions are reported in many other geological environments. For example, in some metamorphic settings, the presence of mineral assemblages stable under low fugacities of O_2 leads to the presence of high proportions of H_2, hydrocarbons and NH_3 (*e.g.*, Agafonov & Andreyeva 1972, Honma & Itihara 1981, Moine *et al.* 1994). However, routine investigation of the inclusion volatiles is typically restricted to analyses of the "common" species, *i.e.*, H_2O, CO_2 and CH_4, because of the difficulty of analyzing gases present in relatively low concentrations. We believe that the gas chromatographic system discussed above offers an inexpensive, easy-to-use method that, if employed routinely, could greatly improve our knowledge of the composition of crustal fluids in a variety of geological settings.

CONCLUSIONS

1. The gas chromatographic system developed for the analysis of fluid inclusions at the Department of Earth and Planetary Sciences of McGill University is based on a system in the Department of Geology at the University of Toronto (*cf.* Bray & Spooner 1989). It is equipped with in series photo-ionization and micro-thermal conductivity detectors. Heated crushing (~120°C) causes immediate release of volatiles, limiting adsorption of gas onto newly created surfaces (*e.g.*, Barker & Torkelson 1975), but the temperature is low enough to avoid chemical reactions among released gases. On-line crushing maximizes the proportion of the released volatiles entering the column, thereby reducing detection limits ($<10^{-4}$ μmoles).

2. We have shown that using a wide-bore capillary column (25 m × 0.53 mm ID fused silica) coated with PoraPLOT® Q greatly improves detection of hydrocarbons over the 10' × $^1/_8$" (3.05 m × 3.2 mm)-OD HayeSep® R packed column, reported to date to be the most efficient column for analysis of fluid-inclusion volatiles. The optimal conditions for analyses using the PoraPLOT® Q capillary column were found to involve a 20-mL/min (at 35°C) carrier-gas flow rate and an oven temperature programmed to start at –20°C, subsequently raised (10°C/min) to 35°C and held for 10 min, then raised again (5°C/min), to 115°C. Runs lasted ~80 min.

3. The capillary column allows analysis for N_2, CO_2, H_2O, CH_4, C_2H_4, C_2H_6, C_2H_2, C_3H_6, C_3H_8 and C_3H_4 to the same or higher degrees of accuracy than with the packed column. Butanes, pentanes and hexanes could not be analyzed or were not detected with the packed column, but produced sharp peaks on the capillary column. Width/height ratios for these gases were of the order of 10^{-5} to 10^{-3}.

4. The samples were analyzed successfully for H_2 and Ar using N_2 as the carrier gas. Detection limits are ~10^{-5} μmoles for H_2, and ~10^{-4} μmoles for Ar. Under these operating conditions, the TCD has lower sensitivity to gases other than H_2, and for obvious reasons, cannot detect N_2. On the other hand, the sensitivity of the PID is relatively unaffected. The results of analyses with N_2 as the carrier gas can be related to those with He as the carrier, by normalizing with respect to CH_4 or C_2H_6.

5. With the capillary column, water produces a peak that has a width/height ratio approximately one quarter that of the peak produced by similar amounts of water analyzed with the packed column. This permits a more precise analysis for H_2O, and lowers the limit for its detection by a factor of about four.

6. Starting the runs at subambient temperatures, combined with the lower retention of H_2O in the capillary column, allowed clean resolution of the propane peak, whereas with the packed column, propane could not be analyzed for owing to interference with the water signal.

7. Aliphatic species heavier than hexane and aromatic

hydrocarbons can be separated on the PoraPLOT® column, but in order to detect these gases at the low levels generally encountered in natural fluids, the oven temperature has to be increased above 115°C, which is the highest temperature at which the system can presently operate.

8. Routine application of this technique should prove to be of great help to most specialists of fluid inclusions dealing with geological problems. For example, analyses of fluid inclusions from the Strange Lake peralkaline pluton by the gas chromatographic system described here has allowed us to recognize that the hydrocarbons that originated from degassing of this pluton, and probably reduced gases in alkaline igneous rocks in general, are formed *via* a Fischer–Tropsch reaction involving hydrogenation of magmatic CO_2 and CO. A similar explanation has been proposed for hydrocarbons produced during serpentinization of ultramafic rocks. Other usages of this technique include determination of redox conditions of ore-forming fluids, and applications to the problems related to the disposal of hazardous waste in evaporite beds.

ACKNOWLEDGEMENTS

We are indebted to C. Bray, University of Toronto, and G. Gauthier of Hewlett-Packard (Canada) Ltd., for their assistance during the construction of the gas chromatographic system. The research was funded by a NSERC research grant, a Lithoprobe grant, and a FCAR team grant, all to the second author. The manuscript benefitted from comments and criticisms from G. Macleod and an anonymous reviewer.

REFERENCES

ABELL, P.I, DRAFFAN, C.H., EGLINTON, G., HAYES, J.M., MAXWELL, J.R. & PILLINGER, C.T. (1970): Organic analysis of the returned Apollo 11 lunar sample. *Proc. Apollo 11 Lunar Sci. Conf.*, 1757-1773.

AGAFONOV, L.V. & ANDREYEVA, G.A. (1972): Gases in the alpine-type ultramafics of the Anadyr–Koryak fold system. *Dokl. Akad. Nauk SSSR* **210**, 232-234.

ANDERSON, R.B. (1984): *The Fischer–Tropsch Synthesis.* Academic Press, New York, N.Y.

ANDRAWES, F.F. & GIBSON, E.K., JR. (1979): Release and analysis of gases from geological samples. *Am. Mineral.* **64**, 453-463.

________, HOLZER, G., ROEDDER, E., GIBSON, E.K., JR. & ORO, J. (1984): Gas chromatographic analyses of volatiles in fluid and gas inclusions. *J. Chromatogr.* **302**, 181-193.

BARKER, C.G. & TORKELSON, B.E. (1975): Gas adsorption on crushed quartz and basalt. *Geochim. Cosmochim. Acta* **39**, 212-218.

BEHAR, F. & PINEAU, F. (1979): Analyse de CO_2, H_2O, hydrocarbures des inclusions fluides par chromatographie en phase gazeuze: application aux fentes alpines et aux roches métamorphiques. *Bull. Minéral.* **102**, 611-621.

BERNDT, M.E., ALLEN, D.E. & SEYFRIED, W.E., JR. (1996): Reduction of CO_2 during serpentinization of olivine at 300°C and 500 bar. *Geology* **24**, 351-354.

BRAY, C.J. & SPOONER, E.T.C. (1989): Fluid inclusion volatile analysis using heated crushing (~105°C)/gas chromatography with in-series photoionization/thermal conductivity detectors and digital peak processing. *Proc. 2nd Biennial Pan-Am. Conf. Res. Fluid Inclusions* **2**, 12-13.

________ & ________ (1992): Fluid inclusion volatile analysis by gas chromatography with photoionization/micro-thermal conductivity detectors: applications to magmatic MoS_2 and other H_2O–CO_2 and H_2O–CH_4 fluids. *Geochim. Cosmochim. Acta* **56**, 261-272.

________, ________ & THOMAS, A.V. (1991): Fluid inclusion volatile analysis by heated crushing, on-line gas chromatography; applications to Archean fluids. *J. Geochem. Explor.* **42**, 167-193.

CHARLOU, J.-L. & DONVAL, J.-P. (1993): Hydrothermal methane venting between 12°N and 26°N along the Mid-Atlantic Ridge. *J. Geophys. Res.* **98**, 9625-9642.

CHOU, I-MING, PASTERIS, J.D. & SEITZ, J.C. (1990): High-density volatiles in the system C–O–H–N for the calibration of a laser Raman microprobe. *Geochim. Cosmochim. Acta* **54**, 535-543.

CUNEY, M., PAGEL, M. & TOURET, J. (1976): L'analyse des gaz des inclusions fluides par chromatographie en phase gazeuse. *Bull. Soc. fr. Minéral. Cristallogr.* **99**, 169-177.

DELHAYE, M. & DHAMELINCOURT, P. (1975): Raman microprobe and microscope with laser excitation. *J. Raman Spectros.* **3**, 33.

DRISCOLL, J.N. & DUFFY, M. (1987): Photoionization detector: a versatile tool for environmental analysis. *Chromatography* **2**, 21-27.

DUBESSY, J. (1984): Simulation des équilibres chimiques dans le système C–O–H. Conséquences méthodologiques pour les inclusions fluides. *Bull. Minéral.* **107**, 155-168.

EUGSTER, H.P. & SKIPPEN, G.B. (1967): Igneous and metamorphic reactions involving gas equilibria. *In* Researches in Geochemistry (P.H. Abelson, ed.) **2**. John Wiley & Sons, New York, N.Y. (492-520).

GERLACH, T.M. (1980): Chemical characteristics of the volcanic gases from Nyiragongo lava lake and the generation of CH_4-rich fluid inclusions in alkaline rocks. *J. Volcanol. Geotherm. Res.* **8**, 177-189.

GOGUEL, R. (1963): Die chemische Zusammensetzung der in den Mineralen einiger Granite und ihrer Pegmatite eingeschlossenen Gase und Flüssigkeiten. *Geochim. Cosmochim. Acta* **27**, 155-181.

Gough, T.A. & Simpson, C.F. (1972): Water adsorption by porous polymer bead gas chromatography columns. *J. Chromatogr.* **68**, 31-45.

Halter, W.E., Williams-Jones, A.E. & Kontak, D.J. (1996): The role of greisenization in cassiterite precipitation at the East Kemptville tin deposit, Nova Scotia. *Econ. Geol.* **91**, 368-385.

________, ________ & ________ (1998): Origin and evolution of the greisenizing fluid at the East Kemptville tin deposit, Nova Scotia, Canada. *Econ. Geol.* (in press).

Heinrich, E.W. & Anderson, R.J. (1965): Carbonatites and alkalic rocks of the Arkansas River area, Fremont County, Colorado. 2. Fetid gas from carbonatite and related rocks. *Am. Mineral.* **50**, 1914-1920.

Hollis, L.O. (1966): Separation of gaseous mixtures using porous polyaromatic polymer beads. *Anal. Chem.* **38**, 309-316.

________ & Hayes, W.V. (1966): Water analysis by gas chromatography using porous polymer columns. *J. Gas Chromatogr.* **4**, 235-239.

Holloway, J.R. (1976): Fluids in the evolution of granitic magmas: consequences of finite CO_2 solubility. *Geol. Soc. Am., Bull.* **87**, 1513-1518.

Honma, H. & Itihara, Y. (1981): Distribution of ammonium in minerals of metamorphic and granitic rocks. *Geochim. Cosmochim. Acta* **45**, 983-988.

Kelley, D.S. (1996): Methane rich fluids in the oceanic crust. *J. Geophys. Res.* **101**, 2943-2962.

Kesler, S.E., Haynes, P.S., Creech, M.Z. & Gorman, J.A. (1986): Application of fluid inclusion and rock-gas analysis in mineral exploration. *J. Geochem. Explor.* **25**, 201-215.

Kogarko, L.N., Kosztolanyi, C. & Ryabchikov, I.D. (1987): Geochemistry of the reduced fluid in alkali magmas. *Geochem. Int.* **24**(7), 20-27.

Konnerup-Madsen, J. (1984): Compositions of fluid inclusions in granites and quartz syenites from the Gardar continental rift province (South Greenland). *Bull. Minéral.* **107**, 327-340.

________, Dubessy, J. & Rose-Hansen, J. (1985): Combined Raman microprobe spectrometry and microthermometry of fluid inclusions in minerals from igneous rocks of the Gardar province (South Greenland). *Lithos* **18**, 271-280.

________, Kreulen, R. & Rose-Hansen, J. (1988): Stable isotope characteristics of hydrocarbon gases in the alkaline Ilímaussaq complex, south Greenland. *Bull. Minéral.* **111**, 567-576.

________, Larsen, E. & Rose-Hansen, J. (1979): Hydrocarbon-rich inclusions in minerals from the alkaline Ilímaussaq intrusion, South Greenland. *Bull. Minéral.* **102**, 642-653.

Kreulen, R. & Schuiling, R.D. (1982): N_2–CH_4–CO_2 fluids during formation of the Dôme de l'Agout, France. *Geochim. Cosmochim. Acta* **46**, 193-203.

Merle d'Aubigné, J. & Guiochon, G. (1970): Etude du comportement thermique des polystyrènes réticules, type porapak. *Chromatographia* **3**, 153-162.

Miller, R.R. (1986): Geology of the Strange Lake alkalic complex and the associated Zr–Y–Nb–Be–*REE* mineralization. *Newfoundland Dep. Mines and Energy, Mineral Develop. Div., Rep.* **86-1**, 11-19.

Mironova, O.F., Naumov, V.B. & Frolov, Ye.V. (1973): Chromatographic determination of the concentration of gases in fluid inclusions. *Geokhimiya* **10**, 1514-1521 (in Russ.).

Moine, B., Guillot, C. & Gibert, F. (1994): Controls of the composition of nitrogen-rich fluids originating from reaction with graphite and ammonium-bearing biotite. *Geochim. Cosmochim. Acta* **58**, 5503-5523.

Nivin, V.A., Devirts, A.L. & Lagutina, Ye.P. (1995): The origin of the gas phase in the Lovozero massif based on hydrogen-isotope data. *Geochem. Int.* **32**(8), 65-71.

Pasteris, J.D., Kuehn, C.A. & Bodnar, R.J. (1986): Applications of the laser Raman microprobe RAMANOR U-1000 to hydrothermal ore deposits: Carlin as an example. *Econ. Geol.* **81**, 915-930.

________ & Wanamaker, B.J. (1988): Laser Raman microprobe analysis of experimentally re-equilibrated fluid inclusions in olivine: some implications for mantle fluids. *Am. Mineral.* **73**, 1074-1088.

Petersilie, I.A. & Sørensen, H. (1970): Hydrocarbon gases and bituminous substances in rocks from the Ilímaussaq alkaline intrusion, south Greenland. *Lithos* **3**, 59-76.

Piperov, N.B. & Penchev, N.P. (1973): A study on gas inclusions in minerals. Analysis of the gases from micro-inclusions in allanite. *Geochim. Cosmochim. Acta* **37**, 2075-2097.

Pollock, G.E., O'Hara, D. & Hollis, O.L. (1984): Gas chromatographic separation of nitrogen, oxygen, argon, and carbon monoxide using custom-made porous polymers from high purity divinylbenzene. *J. Chromatogr. Sci.* **22**, 343-347.

Prohl, H., Siemann, M.G. & Dubessy, J. (1997): The radioactive decay of potassium as a possible source for hydrogen in gas bearing fluid inclusions. *In* Proceedings of the XIV European Current Research on Fluid Inclusions (M.C. Boiron & J. Pironon, eds.). CNRS–CREGU, Vandoevre-lès-Nancy, France (278-279).

ROEDDER, E. (1972): Composition of fluid inclusions. *U.S. Geol. Surv., Prof. Pap.* **440 JJ**.

________ (1990): Fluid inclusion analysis – prologue and epilogue. *Geochim. Cosmochim. Acta* **54**, 495-507.

________ & COOMBS, D.S. (1967): Immiscibility in granitic melts, indicated by fluid inclusions in ejected granitic blocks from Ascension Island. *J. Petrol.* **8**, 417-451.

ROSASCO, G.J., ROEDDER, E. & SIMMONS, J.H. (1975): Laser-excited Raman spectroscopy for nondestructive partial analysis of individual phases in fluid inclusions in minerals. *Science* **190**, 557-560.

SALVI, S. & WILLIAMS-JONES, A.E. (1990): The role of hydrothermal processes in the granite-hosted Zr, Y, REE deposit at Strange Lake, Quebec/Labrador: evidence from fluid inclusions. *Geochim. Cosmochim. Acta* **54**, 2403-2418.

________ & ________ (1992): Reduced orthomagmatic C–O–H–NaCl fluids in the Strange Lake rare-metal granitic complex, Quebec/Labrador, Canada. *Eur. J. Mineral.* **4**, 1155-1174.

________ & ________ (1997): Fischer–Tropsch synthesis of hydrocarbons during sub-solidus alteration of the Strange Lake peralkaline granite, Quebec/Labrador. *Geochim. Cosmochim. Acta* **61**, 83-99.

SMITH, T.J., CLOKE, P.L. & KESLER, S.E. (1984): Geochemistry of fluid inclusions from the McIntyre–Hollinger gold deposit, Timmins, Ontario, Canada. *Econ. Geol.* **79**, 1265-1285.

SOBOLEV, V.S., BAZAROVA, T.YU. & KOSTYUK, V.P. (1974): Inclusions in the minerals of some types of alkaline rocks. *In* The Alkaline Rocks (H. Sørensen, ed.). John Wiley & Sons, New York, N.Y. (389-401).

________, ________, SHUGUROVA, N.A., BAZAROV, L.S., DOLGOV, YU.A. & SØRENSEN, H. (1970): A preliminary examination of fluid inclusions in nepheline, sørensenite, tugtupite and chkalovite from the Ilímaussaq alkaline intrusion, South Greenland. *Medd. Grønland* **181**, 1-32.

THOMAS, A.V., PASTERIS, J.D., BRAY, C.J. & SPOONER, E.T.C. (1990): H_2O–CH_4–NaCl–CO_2 inclusions from the footwall contact of the Tanco granitic pegmatite: estimates of internal pressure and composition from microthermometry, laser Raman spectroscopy, and gas chromatography. *Geochim. Cosmochim. Acta* **54**, 559-573.

WELHAN, J.A. (1988): Methane and hydrogen in mid-ocean-ridge basalt glasses: analysis by vacuum crushing. *Can. J. Earth Sci.* **25**, 38-48.

YPMA, P. (1974): Analysis of fluid inclusions by gas chromatography. *NATO Advanced Study Inst.*, Nancy, N.P. Rep.

ZAJAC, I.S., MILLER, R.R., BIRKETT, T. & NANTEL, S. (1984): Le gîte de Zr, Y, Nb, et Be du complexe alcalin de Strange Lake, Québec–Labrador. *Ministère de l'Energie et des Ressources, Québec*, **DV 84-18**, 127-142.

Received April 4, 1995, revised manuscript accepted November 30, 1997.